Supporting Information

Shola: A 3D porous hydrophobic-oleophilic lignocellulosic material for efficient oil/water separation

Keya Mondal,[a] Kushagra Advani,[a] Snigdha Ghosh,[a] Kadhiravan Shanmugnathan,[b] Goutam Kulsi,[c] Swaminathan Sivaram,[d]* and Sayam Sen Gupta [a]*

[a] Department of Chemical Sciences, Indian Institute of Science Education and Research Kolkata, Mohanpur, 741246, India

[b] Polymer Science and Engineering Division, CSIR-National Chemical Laboratory, Pune 411008, India

[c] ChemActiva Innovations Pvt. Ltd., RISE Foundation IISER, Indian Institute of Science Education and Research Kolkata, Mohanpur, 741246, India

[d] Department of Chemistry, Indian Institute of Science Education and Research Pune, Pune 411008, India

* Corresponding authors: Email- s.sivaram@iiserpune.ac.in; *sayam.sengupta@iiserkol.ac.in*

Materials and methods

Shola is found as a shrub in the wetlands of Eastern India and belongs to the *Aeschynomene* genus. The best quality pith comes from West Bengal, with Kolkata being recognized as the main trade centre for this particular item. In the present investigation, *Shola* aged six months was harvested from Lakshmikantapur (22°06'36"N 88°19'15"E), a village in West Bengal. The collected *Shola* was dried, and the bark, distinguished by its dark brown colour, was separated from the white pith using a blade. Subsequently, the *Shola* pith dried in an oven at 60°C. Following the drying phase, the pith was finely ground to a micron size to facilitate detailed analysis studies. Lifelong LLMG23 Power Pro 500-Watt Mixer Grinder was used for grinding. Sodium hydroxide, hydrochloric acid, chloroform, methanol, 1,2-dichloroethane, and n-hexane were purchased from Merck. All oils, petrol, diesel, and crude oil were received from Haldia Petrochemicals Ltd. Olive, mustard, coconut, and soybean oil were ordered from Fortune®. Sodium hypochlorite and Silicon oil were brought from Sigma Aldrich.

The morphology of the material was analysed by scanning electron microscopy (SEM) using Zeiss DSM 950 and FEI QUANTA 200 3D microscope operating at 10 kV using tungsten filament as the electron source. Solid samples were sputtered with a gold-platinum alloy. X-ray tomography images revealed the structural architecture of the *Shola*. The untreated *Shola* pith and all the fractions obtained from the extraction techniques were characterised using nuclear magnetic resonance spectroscopy (NMR). All ^{1}H NMR and ^{13}C NMR spectra were recorded on a Bruker Spectrometer (400 MHz or 500 MHz), and signals referring to deuterated solvents were reported. Solid-state NMR spectra were recorded using the same instrument. Fourier transform infrared (FT-IR) spectra of the extracted fractions were recorded on a Bruker Optics ALPHA II spectrometer with a universal Zn-Se ATR (attenuated total reflection) accessory. All the data has been reported on a wavenumber (cm^{-1}) scale. Powder X-ray diffraction (PXRD) data were acquired within the 2θ range of 2–80° utilizing a Rigaku MicroMax-007HF, equipped with an intensity microfocus rotating anode serving as the X-ray generator. Cu Kα radiation (α = 1.54 Å) with a Ni filter was employed for the diffraction, and a Rigaku R-axis IV++ detector was used for wide-angle experiments. Size exclusion chromatography was conducted using a 1260 Infinity II HT GPC instrument at Aditya Birla Science & Technology Co. Pvt. Ltd. Prior to the GPC experiments, the sample was solubilized using a LiCl/DMac mixture. TGA was performed using a Mettler-Toledo TG50 and SDT Q600 TG-DTA analyser under a nitrogen (N2) atmosphere. The analysis was carried out within the temperature range of 30°C to 800°C, employing a ramp rate of 10 °C min^{-1}. The hydrophobicity was determined by measuring the contact angle. The contact angle was estimated by the sessile drop method using a Digidrop contact angle meter with an 8 µL water drop size.

Experimental section

Scheme S1. Extraction procedures.

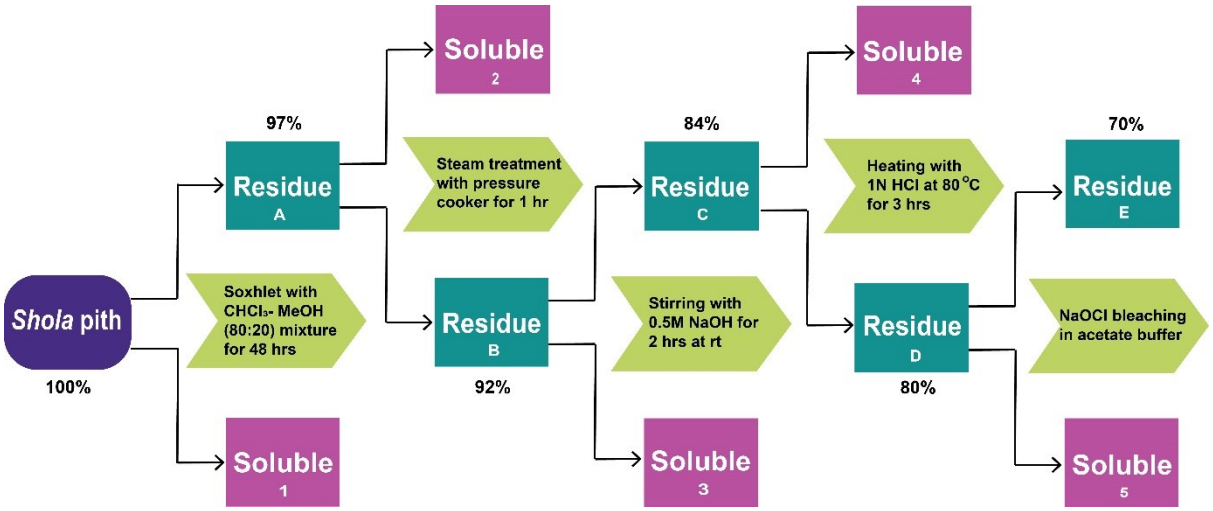

Distinct extraction procedures were employed to isolate components from the *Shola*, excluding the bark. The bark layer was removed from the *Shola* using a blade. The *Shola* pith, ground into a fine powder using a kitchen grinder, was pre-dried at 80°C to eliminate moisture before being subjected to the extraction processes. Fractions obtained through the extraction underwent thorough characterisation utilizing techniques such as NMR, FTIR, GPC, PXRD, TGA, and other analytical methods.

The untreated *Shola* pith:

^{13}C NMR (Solid-state): δ(ppm) 172.33, 152.74, 137.12, 133.11, 105.19, 88.90, 83.85, 74.46, 72.51, 65.03, 56.37, 21.17.

IR ν_{max} (ATR-FTIR)/cm^{-1}: 3345, 2913, 1734, 1640, 1600, 1508, 1369, 1240, 1042, 896.

Extraction of organic solvent-soluble fraction

The dewaxing process of the powdered sample involved exhaustive extraction using a chloroform-methanol mixture (80-20%) in a Soxhlet apparatus for 48 hours. Following the completion of the extraction, the organic solvent fraction was subjected to evaporation, vacuum drying, and subsequent weighing. This fraction (1), identified as the organic-soluble component, was stored and further characterised as the waxy constituent of the *Shola* pith. The post-dewaxing residual solid was vacuum-dried and designated as the dewaxed sample (fraction A) for subsequent investigations.

Fraction 1: 2.5 wt.%

^{1}H NMR (500 MHz, $CDCl_3$): δ(ppm) 7-8, 5.75, 5.32, 3.87, 3.68, 2.37, 2.05, 1.55, 1.28, 0.90, 0.73.

^{13}C NMR (126 MHz, $CDCl_3$): δ 63.54, 31.81, 29.58, 22.57, 14.00, 12.12.

IR ν_{max} (ATR-FTIR)/cm^{-1}: 2922, 2852, 1717, 1508, 1456, 1256, 1088, 1018, 870, 795.

Extraction of water-soluble fraction

A steam explosion process conducted in a pressure cooker was employed to eliminate the water-soluble fraction from the *Shola* pith. In this procedure, 2.5 grams of the dewaxed sample (fraction A) was immersed in 2.5 litres of distilled water and heated in the pressure cooker for one hour. Then, the entire system was promptly cooled and filtered to prevent any defibrillation. The resulting filtrate was concentrated through rotary evaporation at 65°C, followed by further evaporation under vacuum for several hours to eliminate all residual water traces. This water-extracted fraction (2), obtained through hot water treatment, was preserved for subsequent characterisation as the water-soluble component. The remaining solid residue (fraction B) was rinsed with distilled water, dried for mass determination, and utilized in the following extraction procedures.

Fraction 2: 4-6 wt.%

^{1}H NMR (500 MHz, D_2O): δ(ppm) 8.45, 5.19, 4.3-3.3, 3.25, 2.22, 1.90, 1.31.

IR ν_{max} (ATR-FTIR)/cm^{-1}: 3380, 1635, 1388, 1088.

Extraction of base-soluble fraction

One gram of the solid residue (fraction B) underwent extraction using 0.5 M NaOH (25 mL) for 2 hours with continuous stirring at room temperature. Following that, the mixture underwent centrifugation at 10,000 rpm for 15 minutes at 4°C. The resulting supernatant underwent exhaustive dialysis against distilled water for 48 hours, utilizing a 3 kDa dialysis membrane to eliminate the base from the solution. The dialyzed extracted fraction (3) was stored and characterised as the base-soluble component of the *Shola* pith. The residual solid was thoroughly washed with warm water until it reached a neutral pH. The resulting solid residue (fraction C) was then dried for mass determination and utilized in subsequent extraction processes.

Fraction 3: 7-8 wt.%

^{1}H NMR (500 MHz, DMSO-D_6): δ(ppm) 6.70, 4.87, 4.27, 3.07, 1.24.

IR ν_{max} (ATR-FTIR)/cm^{-1}: 3350, 2940, 1734, 1600, 1500, 1230, 1040, 896.

Fraction C:

^{13}C NMR (Solid-state): δ(ppm) 153.64, 137.23, 133.11, 105.34, 88.94, 84.07, 74.80, 72.43, 65.08, 56.24.

IR ν_{max} (ATR-FTIR)/cm^{-1}: 3345, 2912, 1640, 1600, 1508, 1324, 1042, 896.

Extraction of acid-soluble fraction

For the extraction of the acid-soluble component from the *Shola* pith, a 100 mL solution of 1N hydrochloric acid was prepared. The remaining solid (fraction C) was introduced into this acid solution and heated at 80°C with continuous stirring for 3 hours. Subsequently, the mixture was rapidly cooled in an ice-water bath and centrifuged at 10,000 rpm for 15 minutes at 4°C. The resulting supernatant underwent extensive dialysis against distilled water for 48 hours using a 3 kDa dialysis membrane to eliminate the acid from the solution. The dialyzed fraction (4) was preserved for characterisation as the acid-soluble component. The residue was neutralized through multiple washes with distilled water. The resulting solid (fraction D) was then dried for mass determination and employed in subsequent extraction procedures.

Fraction 4: 4-5 wt.%

^{1}H NMR (500 MHz, DMSO-D_6): δ(ppm) 6.70, 5.76, 5.10, 4.23, 3.07, 1.24.

IR ν_{max} (ATR-FTIR)/cm^{-1}: 3370, 2940, 1734, 1600, 1500, 1230, 1045, 896.

Fraction D:

^{13}C NMR (Solid-state): δ(ppm) 153.31, 136.31, 105.25, 89.01, 84.47, 74.96, 72.59, 65.20, 62.83 56.24.

IR ν_{max} (ATR-FTIR)/cm^{-1}: 3345, 2912, 1640, 1600, 1508, 1324, 1042, 896.

Sodium hypochlorite treatment (bleaching)

A bleaching process using NaOCl was employed to separate aromatic components from the *Shola* pith. The residual solid (fraction D) was subjected to treatment at 70°C. for 1 hour using an equal mixture (v/v) of aqueous sodium hypochlorite (1.5 wt.% of NaOCl in water) and acetate buffer (27 g NaOH and 75 mL glacial acetic acid, diluted to 1 L using distilled water). A solid-to-liquid ratio of 1:30 (w/v) was maintained for the bleaching experiment. The bleached solid was filtered, rinsed with deionized water for neutralization, and dried (fraction E). The soluble fraction containing the aromatic component was extracted using chloroform, and the resulting chloroform fraction was dried for characterisation. The residue fraction (E) was stored as the final solid material obtained after the complete extraction process and subjected to characterisation.

Fraction 5: 10-11 wt.%

^{1}H NMR (500 MHz, $CDCl_3$): δ(ppm) 7-8, 5.01, 3.88, 1.41, 1.25, 0.88.

IR ν_{max} (ATR-FTIR)/cm^{-1}: 2924, 2850, 1721, 1600, 1508, 1456,1257, 1021, 796.

Fraction E:

^{13}C NMR (Solid-state): δ(ppm) 105.08, 88.73, 84.13, 74.77, 72.29, 64.92, 62.74.

IR ν_{max} (ATR-FTIR)/cm^{-1}: 3345, 2912, 1640, 1321, 1040, 896.

Quantification of protein

Protein concentration in the *Shola* pith was assessed using two established methods: Lowry's method and the Bradford assay. Both of these protein determination techniques were sensitive to pH variations. All water fractions (2, 3, 4, and 5) obtained from the above-mentioned extraction procedures were collected after careful neutralization through dialysis. Aliquot samples were then diluted using PBS buffer (pH=7.4) for this experimental analysis. A few defined concentrated BSA protein solutions in the same buffer were used as standards. The overall protein content (wt.%) in the pith was determined by summing up the values obtained for each fraction. Each type of experiment was conducted in triplicate for accuracy and reliability.

Characterisation

Organic-soluble fraction (1)

The chloroform-methanol extraction method is widely employed to eliminate waxy constituents from various plant materials[1,2]. The white *Shola* pith reveals an approximately 2.5 wt.% content of the organic solvent-soluble fraction (1) upon gravimetric estimation. Initially, the sample (fraction 1) underwent vacuum drying to eliminate any residual solvent traces and was subsequently reconstituted in $CDCl_3$ for the ^{1}H and ^{13}C NMR spectra recording. In Figure S3, the obtained ^{1}H NMR spectra exhibit prominent peaks within the nonpolar hydrocarbon range of 0.5 to 1.5 ppm, signifying the presence of terminal CH_3/main chain CH_2 groups. Additionally, a few peaks around 4 ppm are observed, primarily originating from methylene (CH_2) groups directly bonded to oxygen (O) atoms in esters. Olefinic peaks are discernible at 5-5.5 ppm, accompanied by aromatic peaks at 7 to 8 ppm. These signals collectively indicate the existence of long-chain hydrocarbons in fatty acids or esters, featuring one or more unsaturation and side group substitutions, a conclusion further supported by the ^{13}C NMR spectra in Figure S4. Signals of significant magnitude observed in the ^{13}C NMR spectra, ranging from 12 to 30 ppm, correspond to long-chain hydrocarbons. The waxy component of the *Shola* pith exhibits peaks akin to those observed for cutin[2,3], a primary polymeric lipid constituent present in plant cuticles. Reported plant waxes predominantly consist of substituted long-chain aliphatic hydrocarbons (paraffin), alkyl esters, fatty acids, fatty alcohols, sterols, ketones, diketones, fatty aldehydes, triterpenoid acids, and other similar compounds. The ATR-FTIR spectra of the waxy constituents reveal numerous stretching signals,[4] indicating a mixture of compounds (Figure S5). The regions around 2922 and 2852 cm^{-1} correspond to -CH_2 antisymmetric and symmetric stretching vibrations, respectively. The peak at 1717 cm^{-1} signifies the C=O stretching mode characteristic of fatty esters. Additionally, the robust signals at 1088 and 1018 cm^{-1} originate from the C-O stretching of alcohol and ether linkages. Other stretching signals at 1456, 1256, and 795 cm^{-1} denote the -CH_2 bending mode vibrations at various structural positions. These infrared stretches further validate the presence of substituted long-chain hydrocarbon structures in the waxy component of the *Shola* pith.

Water-soluble fraction (2)

The steam explosion serves as a conventional approach for extracting water-soluble constituents, including hemicellulose, from plant materials[5]. Utilizing the pressure cooker technique resulted in approximately 5 wt.% of the water-soluble fraction (2), as estimated through gravimetry. The dried sample (fraction 2) was subsequently dissolved in deuterated water (D_2O) for ^{1}H NMR (solvent suppression of water) spectroscopy. In Figure S6, proton peaks falling within the range of 3.00 ppm to 4.00 ppm typically correspond to the xylose and arabinose units of the sugars. Peaks at 1.26 ppm and 1.86 ppm indicate the presence of -CH_3 groups from the acetate group in the side chains, while the peak at 8.42 ppm is associated with the carboxy side chains. Peaks around 5.33 ppm are attributed to anomeric protons of the terminal arabinose moiety. Collectively, these signals represent the hemicellulose backbone of the sugar[6]. In contrast, the ATR-FTIR spectrum of the water-soluble fraction (2) obtained through the steam explosion in Figure S7 displays absorption patterns akin to those reported for hemicellulose[6,7]. Notably, stretching signals at 3300, 2923, 1424, 1044, and 897 cm^{-1} indicate the presence of native hemicelluloses. The broad absorption band at 3380 cm^{-1} is attributed to the hydroxyl group (O-H), while the peak at 2930 cm^{-1} signifies C-H stretching in the -CH_2 groups. The band around 1635 cm^{-1} is associated with the bending of absorbed water. Efforts to eliminate absorbed water from the water-soluble fraction proved challenging, resulting in its persistence as an impurity during characterisation. The peaks at 1388 cm^{-1} denote C-H deformation, and the presence of peaks at 1088 cm^{-1} indicates C-O stretching. The distinctive sharp band at 897 cm^{-1} is assigned to the β-glycosidic linkages between sugar units, which, notably, disappears in fraction 2. This disappearance suggests hemicellulose degradation during the steam explosion treatment.

Base-soluble and acid-soluble fractions (3 and 4)

The *Shola* pith comprises approximately 8 wt.% of a base-soluble fraction (3), as estimated through gravimetry. This fraction appeared as a yellowish colloidal solution in the basic pH and turned white following dialysis. The dialyzed extract underwent drying and redissolving in DMSO-D_6 for the ^{1}H NMR study. In Figure S8, signals in the range of 1-1.5 ppm were observed, indicating the presence of the -CH_3 acetate group. Peaks spanning from 3 to 5 ppm signify the existence of a

sugar backbone. Absorbed water presents as an impurity in the DMSO-D_6 and shows a signal at 3.75 ppm. Aromatic signals between 6.5 to 7.5 ppm potentially originate from aromatic groups.

The acid-soluble fraction (4) comprised approximately 4 wt.%, as determined through gravimetric analysis. Initially displaying an antique-white colloidal solution in the acidic pH, the colour of this fraction transformed to pure white after the dialysis process. Subsequently, the dialyzed extract underwent drying and redissolution in DMSO-D_6 for the ^{1}H NMR study (Figure S10). The proton NMR spectra of both the acid-soluble and base-soluble fractions showed notable similarities, indicating the presence of a sugar backbone with some side chain acetate and aromatic substitutions. Depending on plant sources, hemicellulose and pectin were found to feature acetate and aromatic side chain substitutions, in addition to their primary chain sugar backbone[6,8]. Various studies have explored pectin extraction from plant sources, using different conditions such as pH (1-4), temperature, and extraction duration[9]. In this study, both the acid and base-soluble fractions contained some pectin, with the remaining hemicellulose component of the *Shola* pith. The pectin content was determined separately and discussed below. A notable amount of protein (~ 2 wt.% total) was also detected in the base and acid-soluble fractions.

The ATR-FTIR spectroscopic technique was employed to characterise the dialyzed extractions. In Figures S9 and S11, spectra of the base and acid-soluble fractions (3 and 4) exhibited remarkable similarity. The transmittance band observed at 3370 cm^{-1} was attributed to the stretching of hydroxyl groups. The band at 2940 cm^{-1} corresponded to the stretching vibrations of the C-H group within the glucose unit. The signal at 1043 cm^{-1} was assigned to the C-O group of secondary alcohols and ether functions present in the sugar backbone. The absorption band at 896 cm^{-1}, indicative of the β-glycosidic linkage between glucose units, significantly weakening during the extraction process. The band around 1734 cm^{-1} originated from the carbonyl–carboxyl stretching of the C6 position or side chain. The peaks at 1600 cm^{-1} and 1508 cm^{-1} were linked to the aromatic C=C in-plane symmetrical stretching vibration of the aromatic groups in the side chain substitution. The peak at 1225 cm^{-1} represented the C-O out-of-plane stretching vibration. These stretching frequencies collectively suggested the presence of substituted hemicelluloses and pectin[10] components in the samples.

While handling fractions 3 and 4, some interesting observations were noted. The colloidal extracted solution underwent precipitation and complete phase separation during dialysis. After drying the neutralized solution, the redissolution in DMSO-D_6 for the NMR experiment revealed the formation of a gel to film upon heating-cooling. Pectin is known for its diverse applications as a gelling agent, emulsifier, stabilizer, thickener, and heavy metal adsorbent in various industries such as food, medicine, and cosmetics[11]. Structurally, pectin can undergo methyl esterification with methanol on the carboxylic acid moiety of galacturonic acid or, less commonly, feruloyl-esterification on side chains[8]. The feruloyl group is responsible for little aromatic impurities in the corresponding region of the NMR and IR spectrum. Regrettably, the *Shola* pith exhibited an affinity towards the positively charged molecules compared to negatively charged ones. The native *Shola* pith demonstrated the ability to remove positively charged dye from a water solution and separate positively charged dye from negatively charged dye within a specific concentration range. These observations hypothesized the presence of some pectin component in the *Shola* pith.

Solid residue after NaOH treatment (fraction C)

Initially, the dewax sample underwent treatment with hot water in a pressure cooker, followed by using 0.5N NaOH to remove the base-soluble component. The resulting solid residue (fraction C) was characterised using Solid-state ^{13}C NMR and ATR-FTIR spectroscopic techniques. In Figure S1a, the obtained ^{13}C NMR spectrum has signature peaks of the carbohydrate backbone (50–115 ppm) that remained unchanged compared to the native sample. However, the additional peak at 22 ppm and the broad peak at 173 ppm, representing the acetyl and carbonyl groups, respectively, vanished completely. Notably, some undesired signals persisted, including a sharp peak at 56 ppm representing the methoxy carbon of aromatic conjugation, two overlapped peaks at 133-137 ppm representing aromatic C=C carbons, and a strong peak at 152 ppm representing phenolic carbon. Notably, the intensity of these peaks did not change from the native *Shola* sample. These results indicate the presence of aromatic groups as a component in the sample, strongly attached to the cellulosic component of the *Shola* pith. Moreover, the ATR-FTIR spectrum of the residue fraction C yielded similar outcomes (Figure S2a). The bands at 1734 cm^{-1} for carbonyl stretching and 1240 cm^{-1} for the C-O out-of-plane stretching vanished completely. However, bands at 1600 cm^{-1} and 1508 cm^{-1} representing aromatic bond stretches remained unchanged. All other cellulosic signals remained consistent with the spectrum of the native *Shola* pith. Consequently, additional treatments were deemed necessary to eliminate the remaining aromatic components from the sample.

Solid residue after HCl treatment (fraction D)

To eliminate acid-soluble components, the residue solid (C) underwent additional treatment with 1N hydrochloric acid. Although a slight mass loss (4-6 wt.%) was observed in this step, both Solid-state ^{13}C NMR and ATR-FTIR spectra of residue fraction D closely resembled those of the previous NaOH-treated residue solid (C). Aromatic peaks persisted without any change in the samples even after acidic extraction (Figure S1b & S2b). Consequently, further treatment was undertaken with the residue to address this issue.

Bleach extracted fraction (5)

The use of sodium hypochlorite treatment is widely recognized for eliminating aromatic impurities, particularly lignin, from plant materials[12]. Lignin is a polymer made up of phenylpropane units, which are derived from hydroxyl- and methoxy-substituted phenylpropane units. Typically, the reported lignin compounds exhibit dark yellow or brown hues, resembling the colour of the bark in the *Shola*. However, in our current study, the bleach extraction fraction (5) of the white pith appeared yellowish. The *Shola* pith was determined to contain approximately 10 wt.% of the NaOCl extractable fraction (5), as estimated through gravimetric analysis. Following NaOCl treatment, the dialysis step was intentionally omitted to prevent the loss of any small aromatic groups from the extracted solution. For characterisation, purification was carried out utilizing the organic solvent chloroform. The NaOCl-soluble fraction was extracted using chloroform to transfer aromatic compounds into the organic solvent layer. The chloroform fraction was dried and redissolved in $CDCl_3$ for the ^1H NMR study. The resulting spectra in Figure S12 exhibited prominent signals in the 1 to 1.5 ppm region, indicative of the $-CH_3$ acetate group, along with some shifts in the 6 to 7.5 ppm aromatic region.

The ATR-FTIR spectra of the bleached extracted portion exhibited distinct differences compared to the spectra of other extractive fractions (Figure S13). Notably, the NaOCl-extracted fraction displayed highly intense transmittance band peaks at 2934 cm^{-1}, corresponding to the stretching of C–H bonds in the methyl and methylene groups within the side chains of aromatic groups. Additionally, the bands at 2860 cm^{-1} were attributed to the C–H stretching in the aromatic methoxyl moieties. A robust signal at 1721 cm^{-1} indicated the stretching of the acetyl substitution. Furthermore, a weak band at 1257 cm^{-1} was assigned to the side-chain vibrations. A weaker symmetric stretching band near 1457 cm^{-1} was observed for carboxylate groups. The peaks at 1600 cm^{-1} and 1508 cm^{-1} were linked to the aromatic C=C in-plane symmetrical stretching vibration. Absorption bands at 1093 cm^{-1} and 1021 cm^{-1} originated from in-plane C-H bending. Notably, all signals related to the cellulosic backbone were absent in this NaOCl-extracted fraction, indicating the presence of a poly-aromatic backbone associated with the lignin[13] component of the *Shola* pith.

The final remaining residue (fraction E)

Following the isolation of all components from the *Shola* pith, a brownish-white colour insoluble solid residue remained. This extracted solid fraction (E) constituted approximately 70 wt.% and underwent characterisation using solid-state ^{13}C NMR and ATR-FTIR spectroscopic techniques. The obtained ^{13}C NMR spectra exhibited a complete match with the reported cellulose[14]. In Figure 3c, the cellulose resonance signals at different carbon positions were identified at 105 ppm (C1), 89 ppm (C4), 73 ppm (C2, C3, C5), and 65 ppm (C6) with intensities nearly similar to those of the untreated sample. Additionally, the crystallinity of the material increased after treatment, as evidenced by changes in the intensity difference between the peaks at 84 ppm and 89 ppm. However, other non-cellulosic peaks associated with aromatic moieties, carbonyl, and acetyl groups of hemicellulose and pectin components vanished entirely from the spectrum. These results demonstrate that hemicellulose, lignin, and other components were isolated successfully, and the final solid residue left was composed of pure cellulose. On the other hand, the FTIR spectrum of the extracted cellulose (fraction E) perfectly aligns with commercial microcrystalline cellulose. Furthermore, identical acquisition parameters were employed to obtain these spectra, and the same sample quantity was utilized to facilitate a more accurate comparison of the resulting spectra changes. In Figure 3d, the absorption band at 3343 cm^{-1} represents the stretching of hydroxyl groups, while bands at 2912 cm^{-1} and 1369 cm^{-1} were designated for the stretching and deformation vibrations of the C-H bonds within the glucose unit. The peak at around 1640 cm^{-1} indicates the O-H bending vibration of absorbed water. Although all samples were carefully dried before testing, eliminating absorbed moisture in cellulose molecules proved challenging due to cellulose-water interaction. The absorption band at 896 cm^{-1} is characteristic of the β-glycosidic linkage between glucose units, and the band at 1040 cm^{-1} is attributed to the C-O group of secondary alcohols and ether functions in the cellulose chain backbone. All these signals further prove the intact bonding of the cellulosic backbone after the aforementioned extraction process. However, in comparison to the native sample, the absorption band at 1734 cm^{-1} corresponding to C=O stretching vibration vanished. The peak at 1240 cm^{-1}, representing the C-O out-of-plane stretching vibration, had disappeared completely. It was hypothesized that these disappearances were linked to the carboxylic groups present in the hemicellulose and pectin's side chain. Bands at 1602 cm^{-1} and 1508 cm^{-1} associated with the aromatic C=C were also removed. The absence of all these peaks from the extracted final residue further confirmed its cellulosic purity.

Pectin estimation by Gravimetric method

Further, we estimated the amount of pectin present in the *Shola* pith using a conventional method reported for pectin extraction from other biosources[9]. After dewaxing and hot water treatment, the residue sample was subject to acid extraction. 1 g of the sample (fraction B) was dispersed in 100 mL of a solution of 3% (v/v) acetic acid**.** Then, pectin extraction was performed at 90°C for 6 hours under a magnetic stirrer. Afterward, the suspension obtained was rapidly cooled to room temperature and filtered to separate the liquid extract from the insoluble fraction. Once the liquid fraction was recovered, the pectin was precipitated with an excess of isopropanol (twice the volume with respect to the liquid extract volume) and filtrated using filter paper. The pectin was washed with ethanol and put into a vacuum oven at 60 °C until reaching a constant weight. This experiment was repeated three times, and the analysis results demonstrated 2-3 wt.% of pectin in the sample gravimetrically.

Quantification of protein

Protein, a compositional component present in nearly every plant, was found in varying quantities based on the nature of the plant material[15]. The protein content in the *Shola* pith was quantified using both Lowry's method and the Bradford assay. The Lowry method, while sensitive to low concentrations of protein, had the drawback of potential interference from various compounds, including sugars and lipids. To address this, aliquot samples from each solution fraction were diluted (10X) with PBS buffer (pH=7.4) before conducting the Lowry assays. The three water fractions (2, 3, and 4) obtained by extraction were taken for protein estimation. The total protein content was estimated to be approximately 2.11 wt.% using Lowry's method. On the other hand, protein in the extracted solutions was also quantitatively measured through the Bradford assay. Given the assay's sensitivity to pH, aliquot samples were carefully neutralized and diluted (10X) using PBS buffer (pH=7.4). According to the Bradford assay, about 1.9 wt.% of protein was identified as a chemical component in the *Shola* pith.

X-ray diffraction analysis

Cellulose typically comprises a crystalline phase and an amorphous phase[16]. To investigate the structural differences between the untreated *Shola* pith and the extracted cellulose, X-ray diffraction was conducted in powder form. The results (Figure S14a) revealed a well-defined prominent peak around 2θ=22° in both patterns. Additionally, a shoulder at 16° was observed in the extracted cellulose (fraction E). These findings indicated that the native pith exhibited characteristics of cellulose type I. However, the extracted cellulose (Figure S14b) demonstrated characteristics of Cellulose II, which resulted from the treatments involving the use of a high concentration of alkalis. The enhanced crystallinity observed in the extracted cellulose may be attributed to the robust alkaline treatment, which removed hemicellulose, and the potent oxidizing properties of sodium chlorite, which could partially disrupt the intermolecular or intramolecular hydrogen bond network during the removal of aromatic components, leading to the rearrangement of cellulose chains. In X-ray diffraction analysis, peak intensity at a 2θ angle close to 22° indicates crystalline material, while the counter reading at peak intensity at a 2θ angle close to 18° corresponds to amorphous material. The narrow and sharper peak at 22° in the pattern of extracted cellulose reflects a higher crystallinity index (~45%) compared to the native sample (~16%), signifying the elimination of non-cellulosic substances including hemicellulose, lignin, and other impurities. This increased crystallinity percentage in extracted cellulose defines its purity. The crystallinity index (CrI) was estimated using the following equation

$$\mathrm{CrI}(\%) = \frac{\mathrm{I_{cr}} - \mathrm{I_{am}}}{\mathrm{I_{cr}}} \times 100$$

Where, I_{am} is the minimum diffraction intensity (background) at 2θ angle close to 18°, and I_{cr} is the maximum diffraction intensity at 2θ angle close to 22°.

Size Exclusion Chromatography

Size exclusion chromatography, a well-established technology, provides comprehensive insights into the molecular weight distribution of cellulosic polymers. In general, cellulose from natural sources shows a molecular weight range from 50,000 g/mol to more than 500,000 g/mol[17]. Determining the molecular weight of native *Shola* pith is challenging due to its difficulty in dissolution and the presence of interfering non-cellulosic components. To measure the dispersity (Đ) of the extracted cellulose, initial solubilization was performed using an ionic salt and organic solvent mixture. The extracted cellulose (fraction E) showed solubility in the LiCl/DMAc system. The poly was calculated by dividing the weight-average molecular weight (M_w) by the number-average molecular weight (M_n). The obtained M_w was 247,914 g/mol, and M_n was 20,358 g/mol for the extracted cellulose, resulting in a Đ of 12.18. These results (Figure S15) indicate that cellulose extracted from the *Shola* pith possesses a branched polymeric structure of polysaccharides with a high molecular weight.

Thermogravimetric analysis

To assess the thermal stability of the native *Shola* pith and extracted cellulose (fraction E), TGA analysis was conducted from 30 °C to 600 °C with a rate of 10 °C/min. The primary structural components of plants, including cellulose, hemicellulose, pectin, wax, and lignin, decompose at different temperatures due to variations in their chemical structures. According to reports, cellulose typically initiates decomposition at 315 °C, persisting until 400 °C, with the maximum weight loss rate observed at 355 °C[18]. The obtained curves (Figure S16) reveal that the untreated *Shola* pith remains stable up to 200°C, after which decomposition commences above 200 °C, reaching its maximum weight loss at 315 °C. This behaviour is attributed to the decomposition of amorphous non-cellulosic components at lower temperatures. The reduction of these components from the cellulosic component results in decomposition at higher temperatures. The extracted cellulose (fraction E) exhibits decomposition above 300 °C. The removal of non-cellulosic components, such as hemicellulose, lignin, and other impurities, through the applied treatments, contributes to a denser and more compact structure in the extracted cellulose. Enhanced structural integrity and crystallinity of the extracted cellulose lead to improved thermal stability compared to untreated *Shola* pith.

Scanning Electron Microscopy (SEM)

The *Shola* pith exhibits significant hollowness and structured porosity, which is inherently hierarchical. The pith features rectangular interconnected pores ranging from 20 to 30 µm in diameter, within which smaller pores of diameters between 200 nm and 4 µm were found (Figure S17a). For the experimental purpose, the *Shola* pith was ground to micron-sized

powder using a kitchen grinder. In the untreated state, the powder sample maintains its porous structure, with intact small pores (Figure S17b). Nevertheless, the porous structure undergoes alterations post-treatment. Following the dewaxing process, the wet sample underwent natural drying at room temperature through the evaporation of the employed organic solvent. Interestingly, compression in the size of the sample occurred during this evaporation phase, while the porous structure remained unaltered. Subsequently, a similar phenomenon was observed in the solid residue samples after hot water extraction. Notably, after undergoing base/acid treatment, the structure collapsed, and the smaller pores disappeared. Further bleach treatments caused the spongy structure to collapse completely, leading to an increase in the density of the solid residue (Figure S17c). In the final extracted cellulose, there was a complete absence of pores, giving it a more fibrous appearance.

Mechanical strength

For a reusable material to be practically exploitable in any application, mechanical properties are crucial. To assess the material's strength, compressive stress-strain behaviour was analysed. The mechanical properties of the *Shola* pith were evaluated using a Universal Tensile Testing Machine UTM33R with load cell 1 kN and compression rate 5 mm/min. For this experiment, a cylindrical-shaped native *Shola* pith sample of 5 mm in height and 30 mm in diameter was used. The results showed a high compressive stress of 695 kPa and a modulus of 2.1 MPa. The obtained stress-strain curve is shown in Figure S22.

Anti-corrosive properties

The robustness of *Shola* pith in corrosive liquids and tolerance to continuous contact with extremely corrosive solutions was checked. Two independent methods were employed to assess the changes in hydrophobic properties of the *Shola* pith due to exposure to a strong acid or alkali. 0.1N HCl (pH = 1) and 1N NaOH (pH = 14) were used as the acidic and alkaline solutions, respectively, and DI water was used as a control. In the first method, the sample was soaked in water, HCl, and NaOH solutions for a specific period of 1 hr, 2 hr, and 4 hr. After the set immersion time, the sample was removed from the corrosive liquids and dried at 60°C. Subsequently, a water droplet was placed on the surface to examine the effect of the corrosive solution on wettability. In the second method, the acidic, alkaline, and water droplets were applied to the native *Shola* pith surface, and the change in contact angle was monitored over time to study how the corrosive liquid influenced the wettability. For the first one, after dipping in the basic solution, the water droplet was spread out on the surface of the dried sample, and the contact angle significantly decreased compared to the native *Shola* pith (Figure S23a). On the other hand, after dipping in the HCl solution, no significant change in the water contact angle on the dried sample was observed, and the water remained as a droplet. The same thing was observed in the case of the dried sample, dipped in DI water. Notably, samples dipped for longer (4 hrs) show similar results. In the drying process, during evaporation of the sorbed alkaline solution, the 3D porous structure of the *Shola* pith collapses. However, it is believed that the immersion method may not fully capture the intricacies of superhydrophobic degradation, as the degradation mechanism involves the hydration of surface-active sites, which tends to form hydrogen bonds ref. In the second method, the alkaline drop was spread out slowly, but acidic and normal water remained as droplets on the native *Shola* pith (Figure S23b). After 3-4 hrs, the NaOH solution was fully sorbed by the sample, and after drying, that small area of the pith collapsed like a cavity. This is probably because the NaOH solution can rupture the complex lignocellulosic structure by hydrolysing hemicellulose, and strong alkali can weaken the β-sheet structure of cellulose by breaking the strong hydrogen bonding between the polysaccharide chains, and thus, water gets entrapped. In the case of HCl and DI water, the droplets did not spread and evaporated slowly without any changes in the sample surface, indicating excellent robustness of the *Shola* pith in an acidic atmosphere.

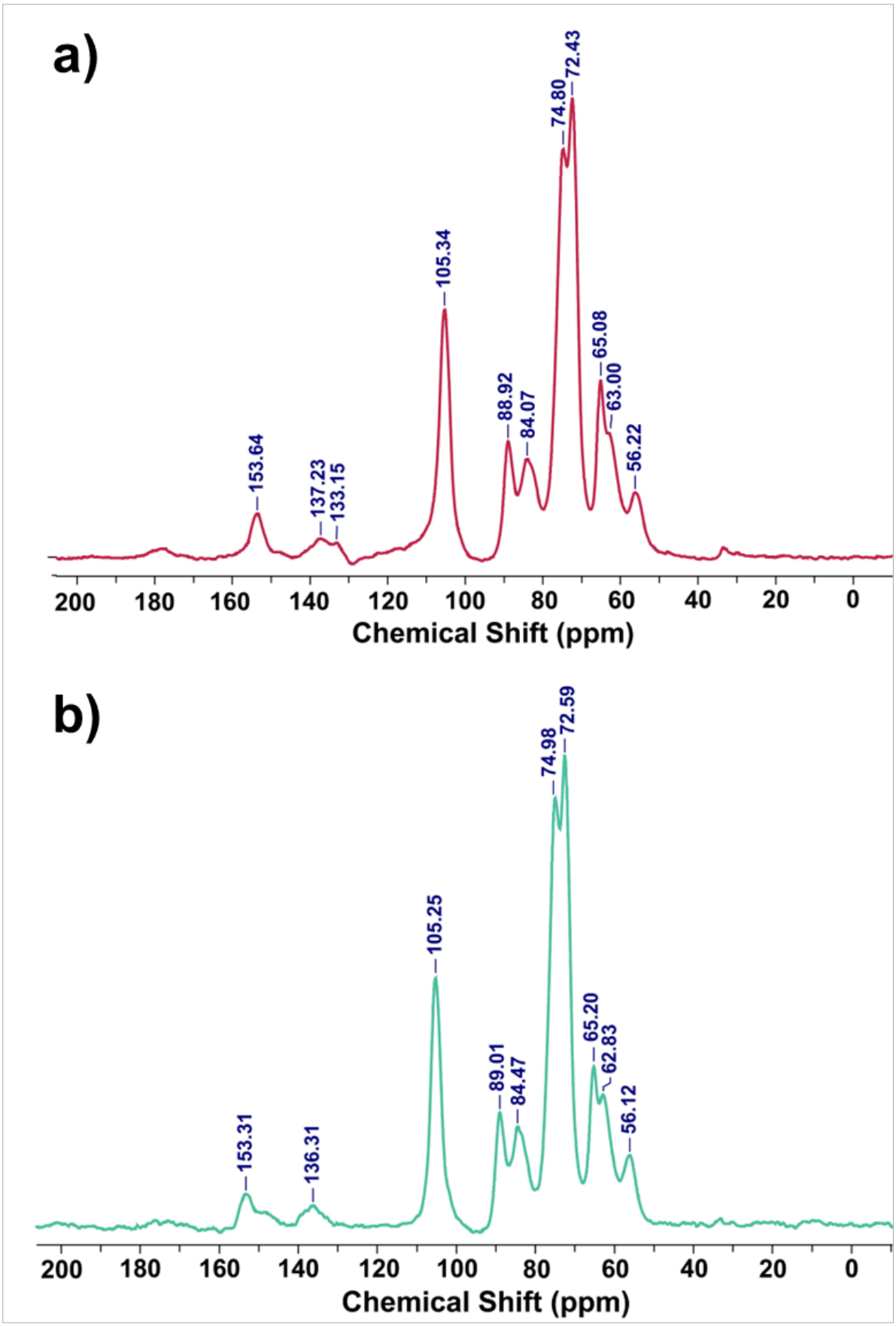

Figure S1. Solid-state ^{13}C NMR spectrums of (a) fraction **C** and (b) fraction **D.**

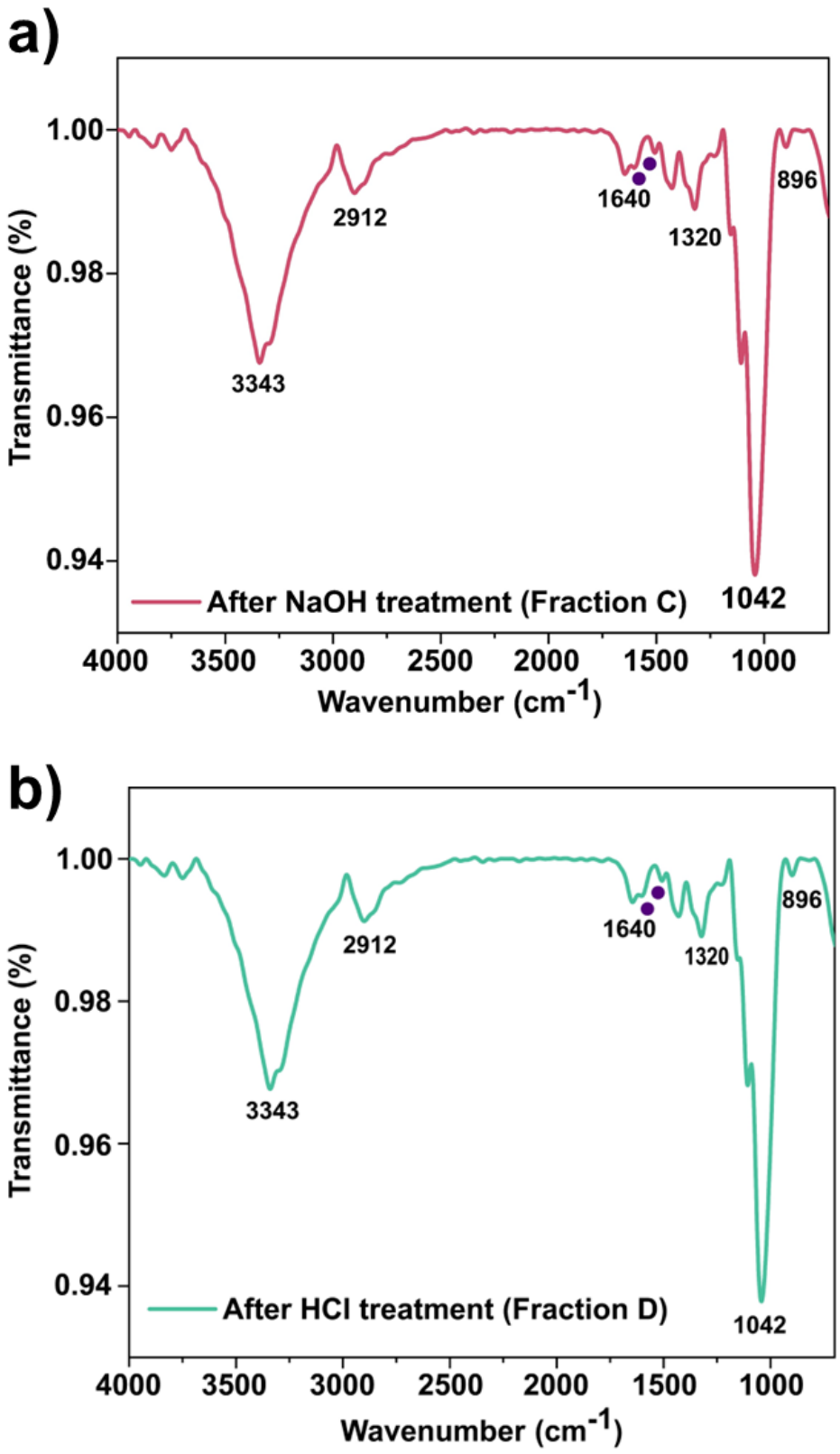

Figure S2. ATR-FTIR spectra of (a) fraction **C** and (b) fraction **D.**

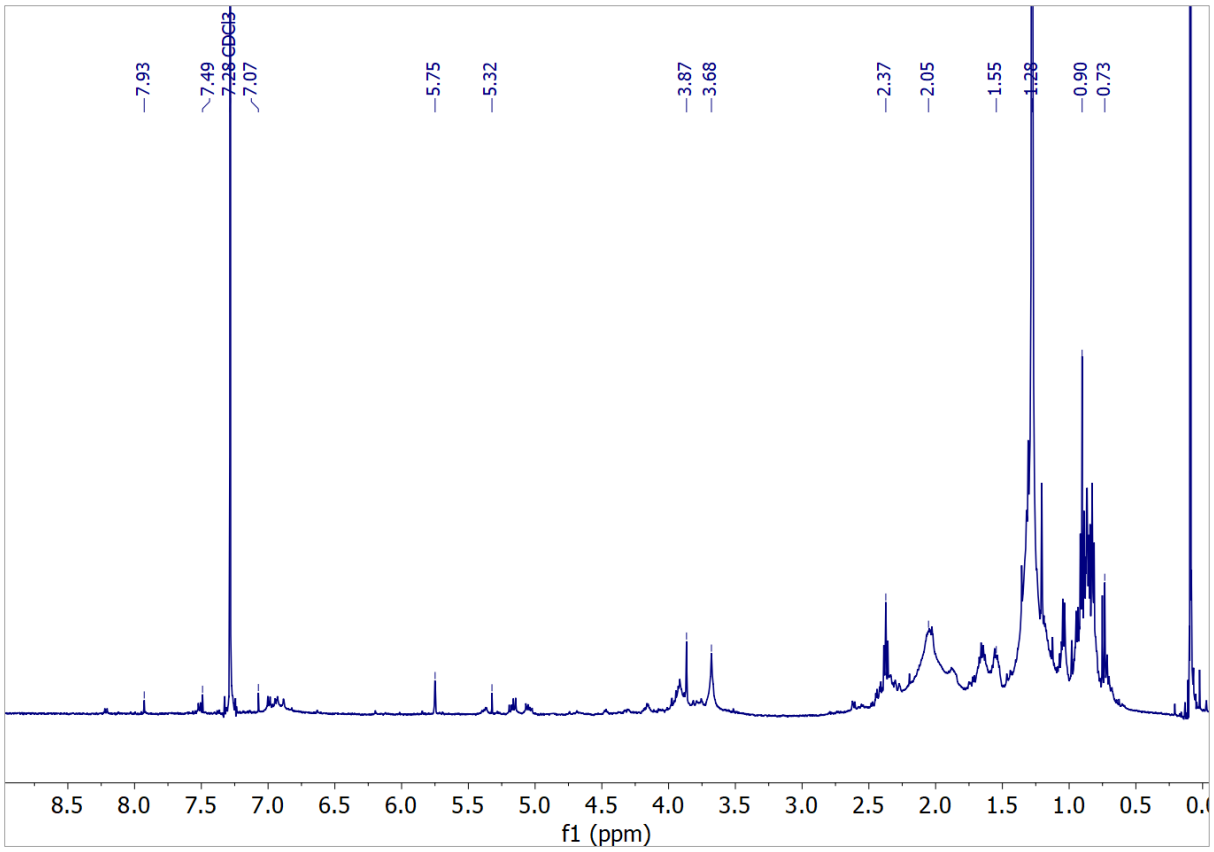

Figure S3: ^{1}H NMR of fraction **1** in $CDCl_3$.

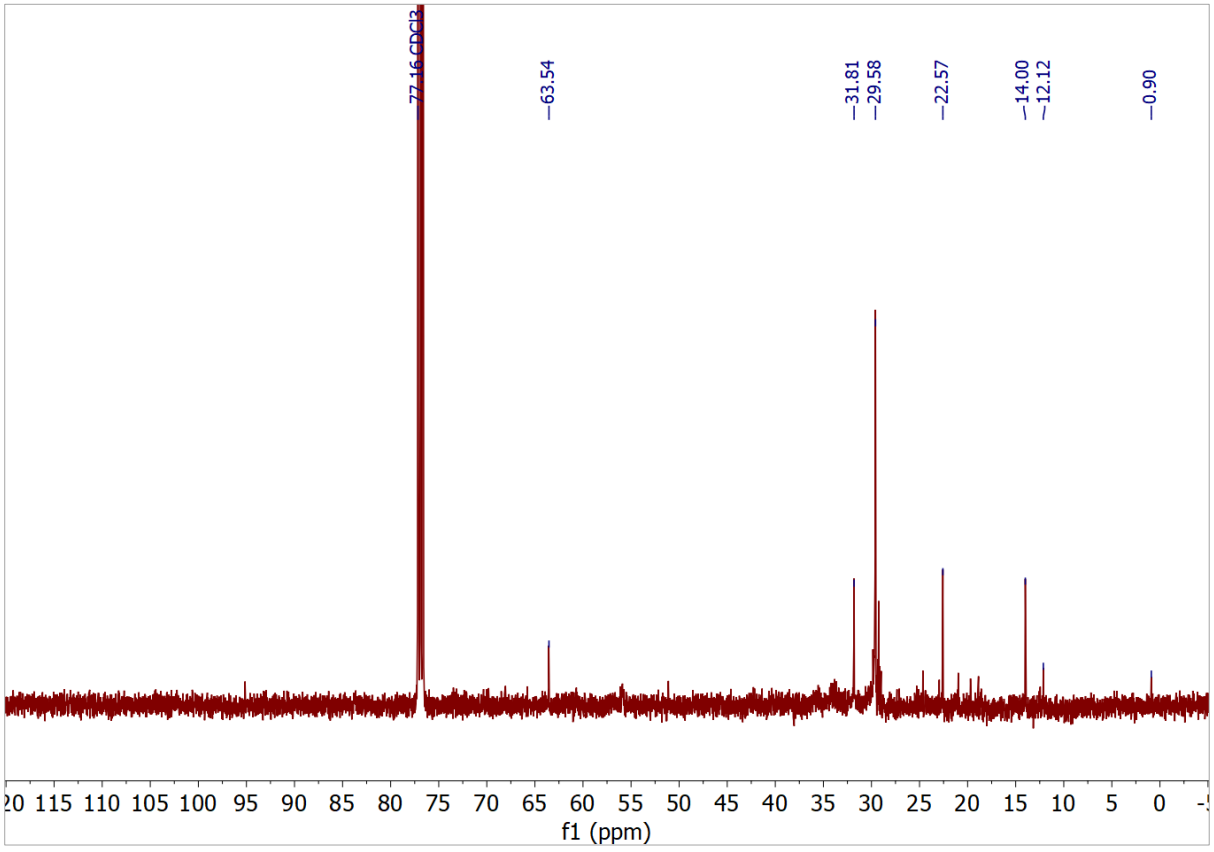

Figure S4: ^{13}C NMR of fraction **1** in $CDCl_3$.

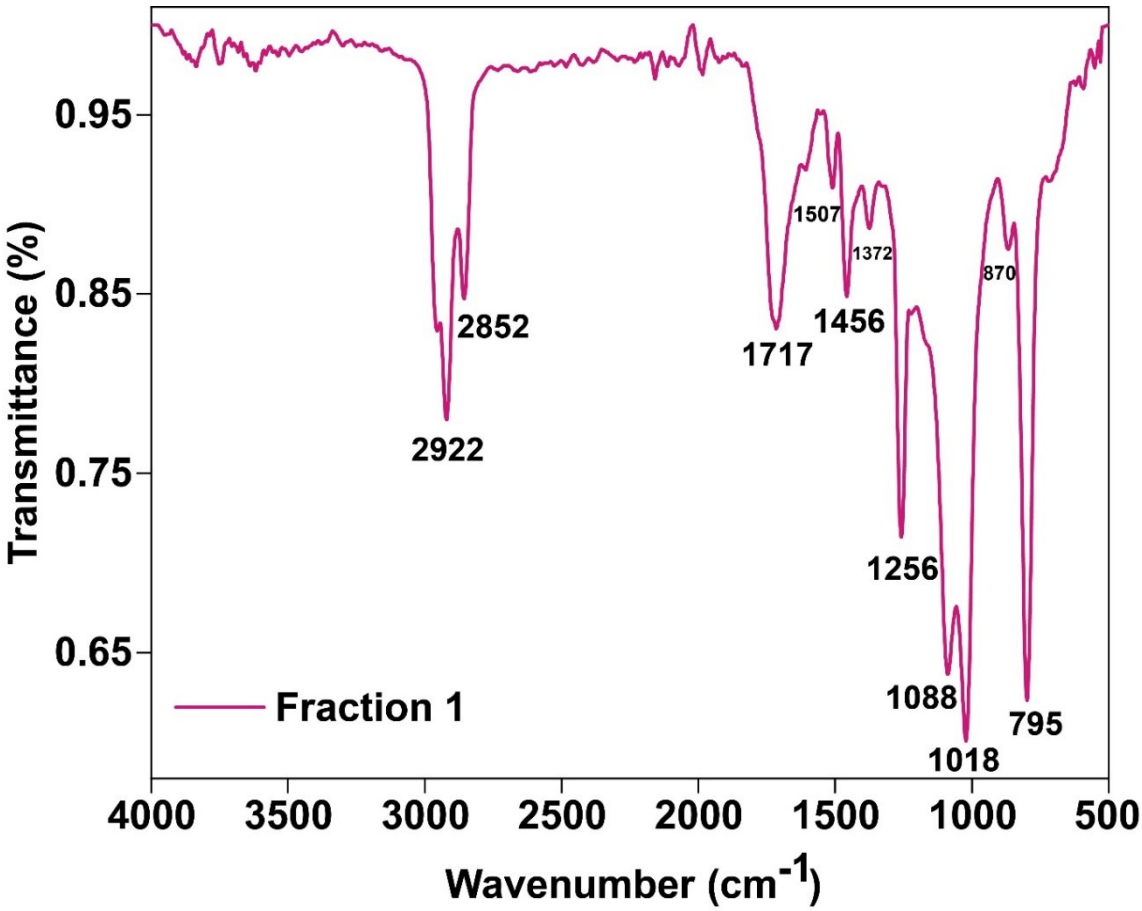

Figure S5: ATR-FTIR of fraction **1** in solid state.

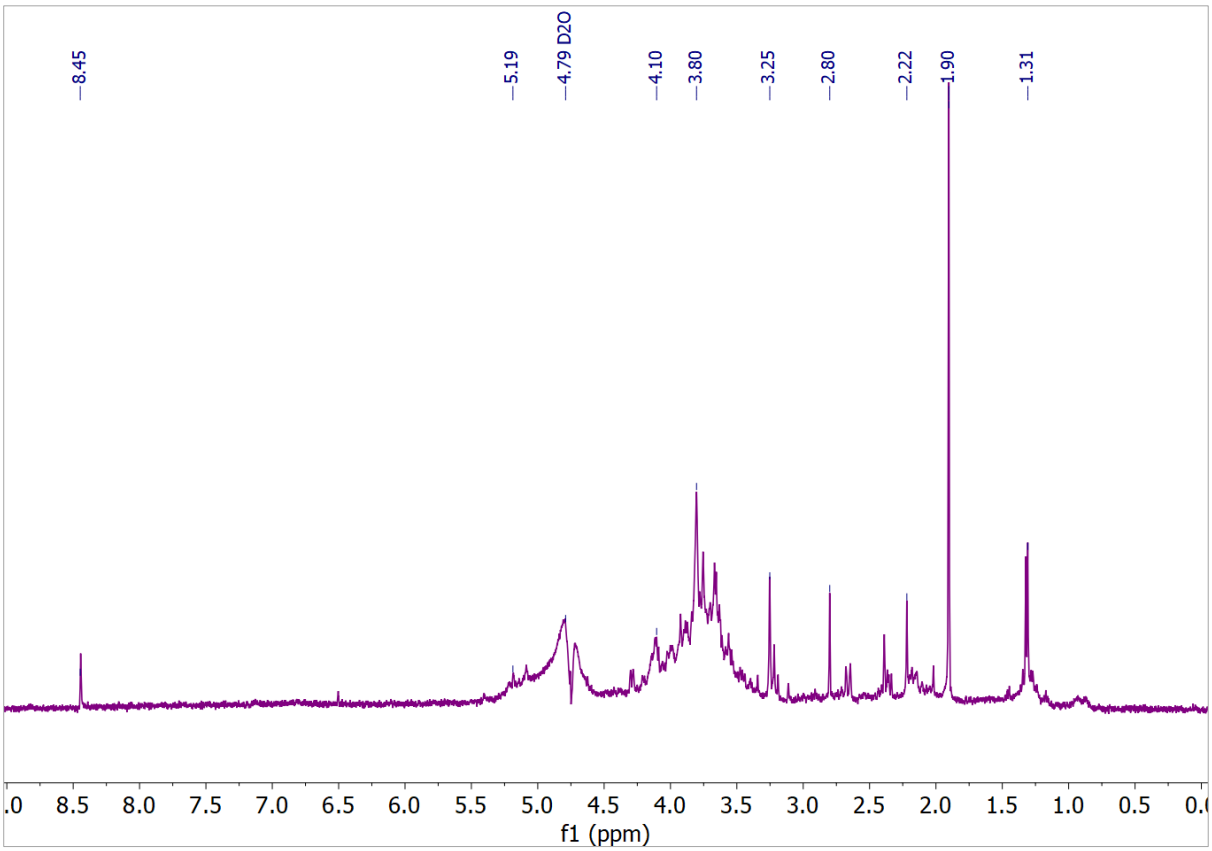

Figure S6: ^{1}H NMR of fraction **2** in D_2O.

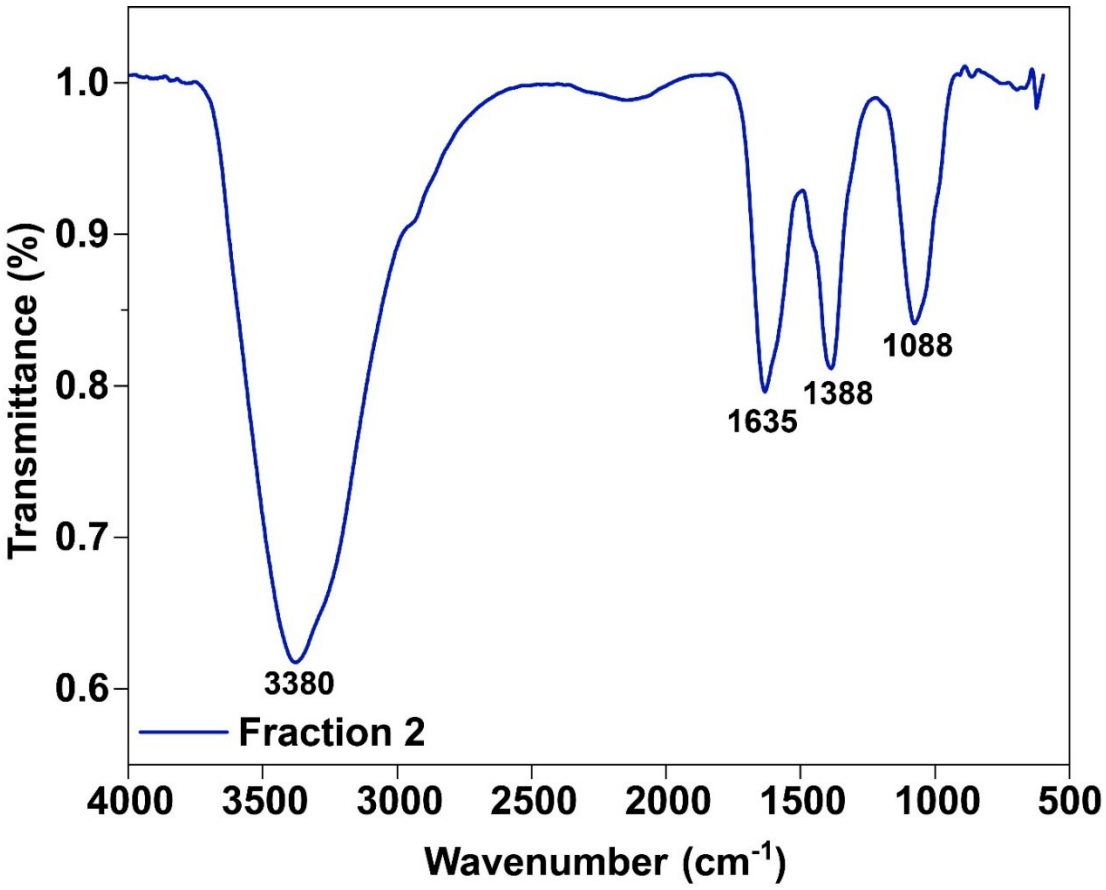

Figure S7: ATR-FTIR of fraction **2** in solid state.

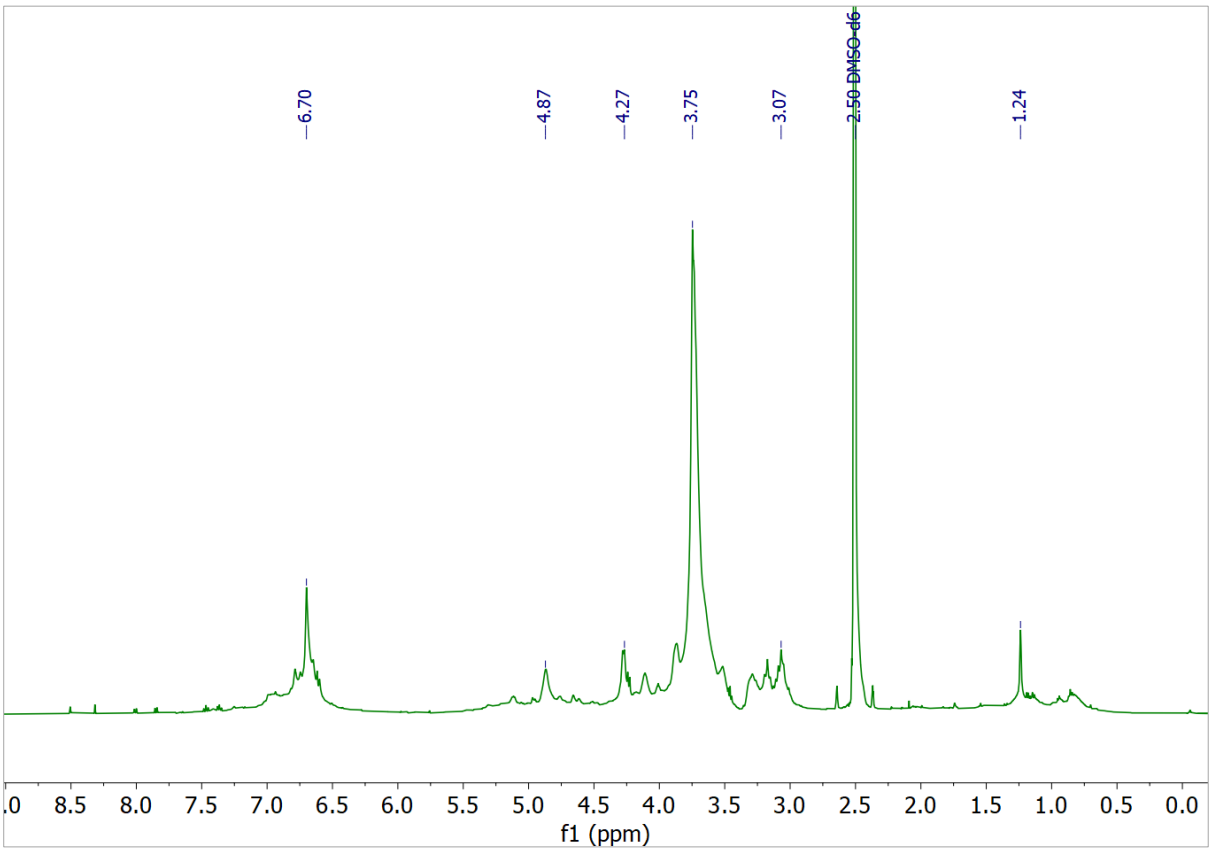

Figure S8: ^{1}H NMR of fraction **3** in DMSO-D_6.

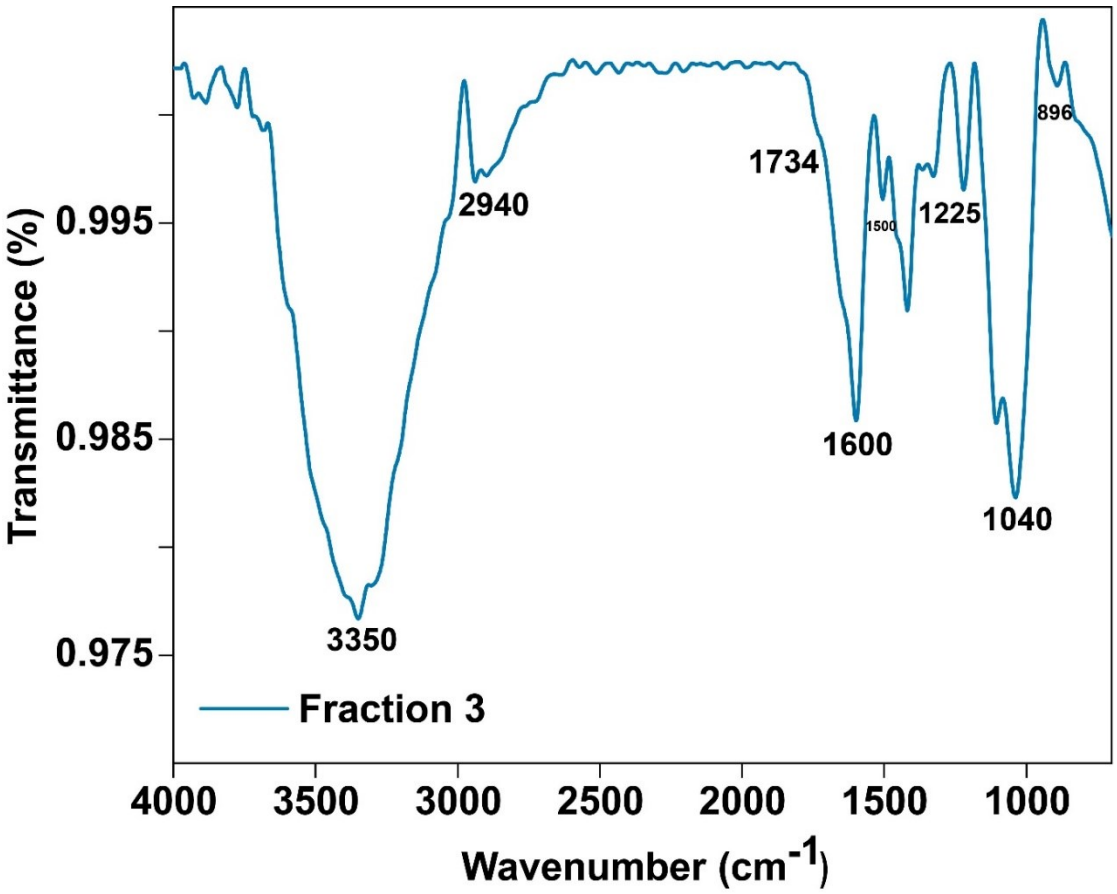

Figure S9: ATR-FTIR of fraction **3** in solid state.

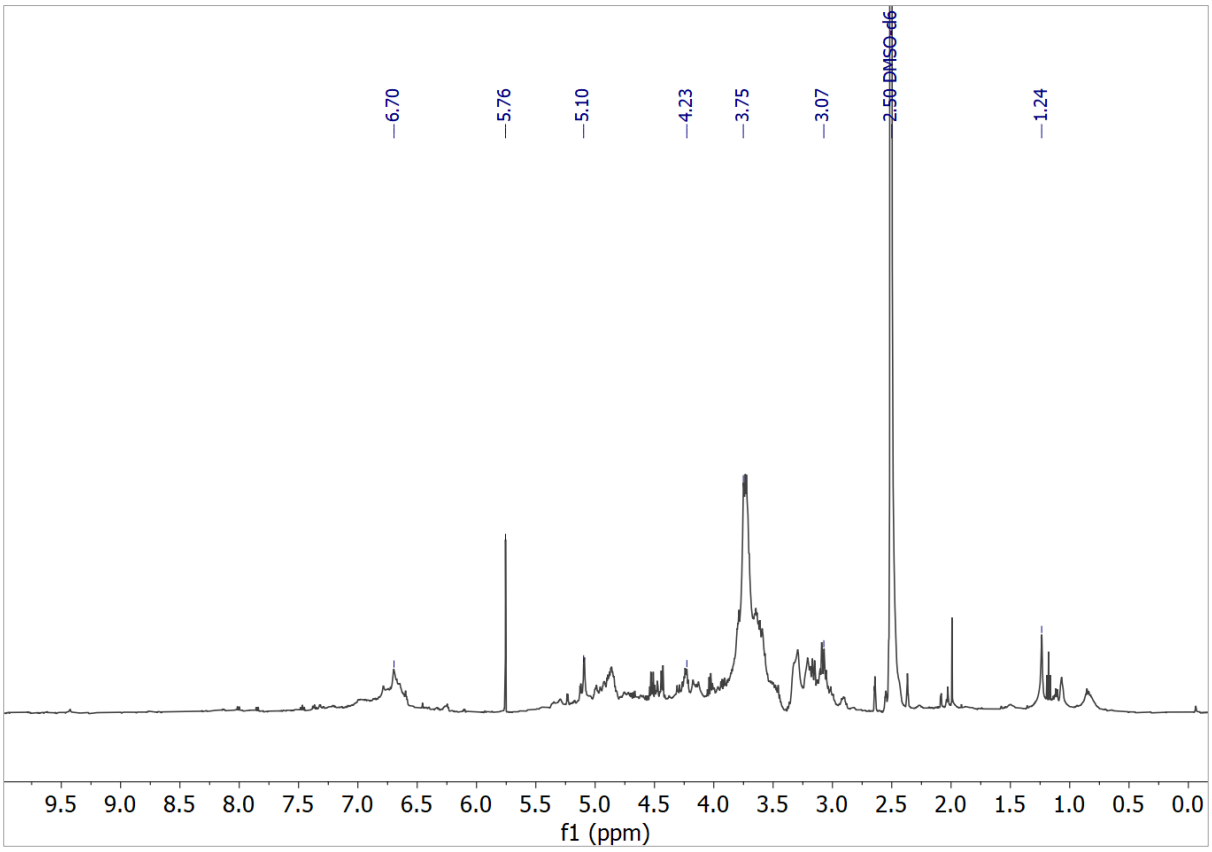

Figure S10: ^{1}H NMR of fraction **4** in DMSO-D_6**.**

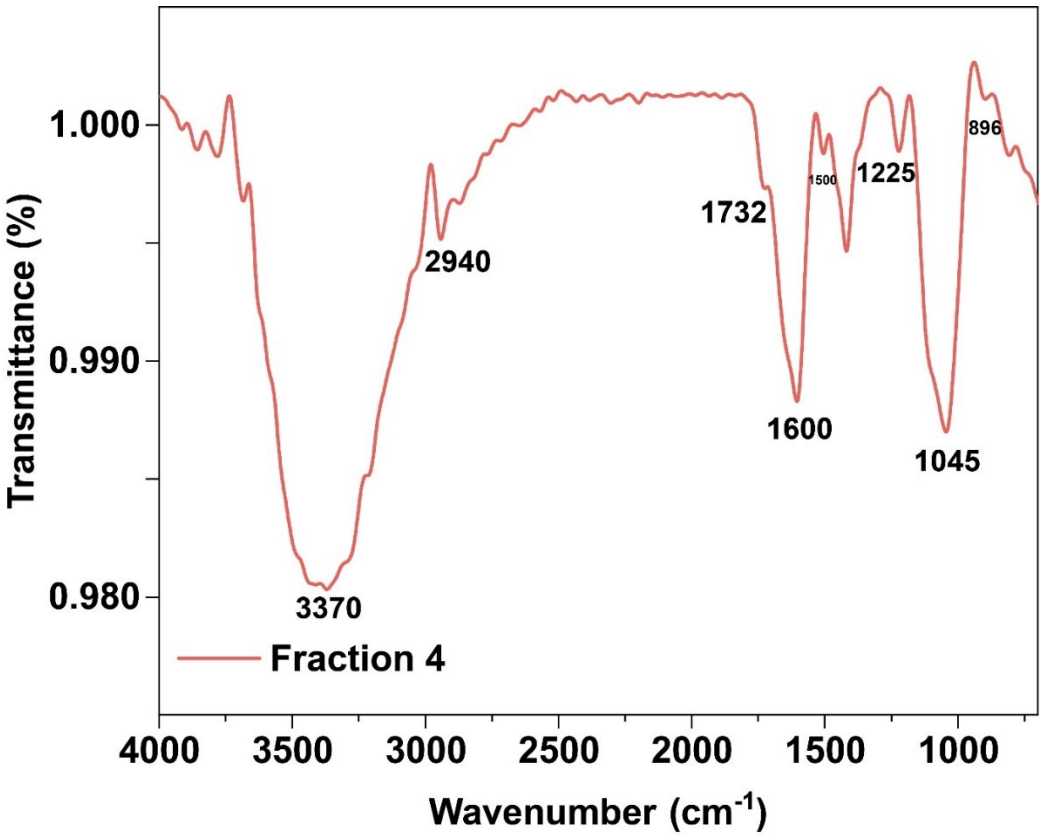

Figure S11: ATR-FTIR of fraction **4** in solid state.

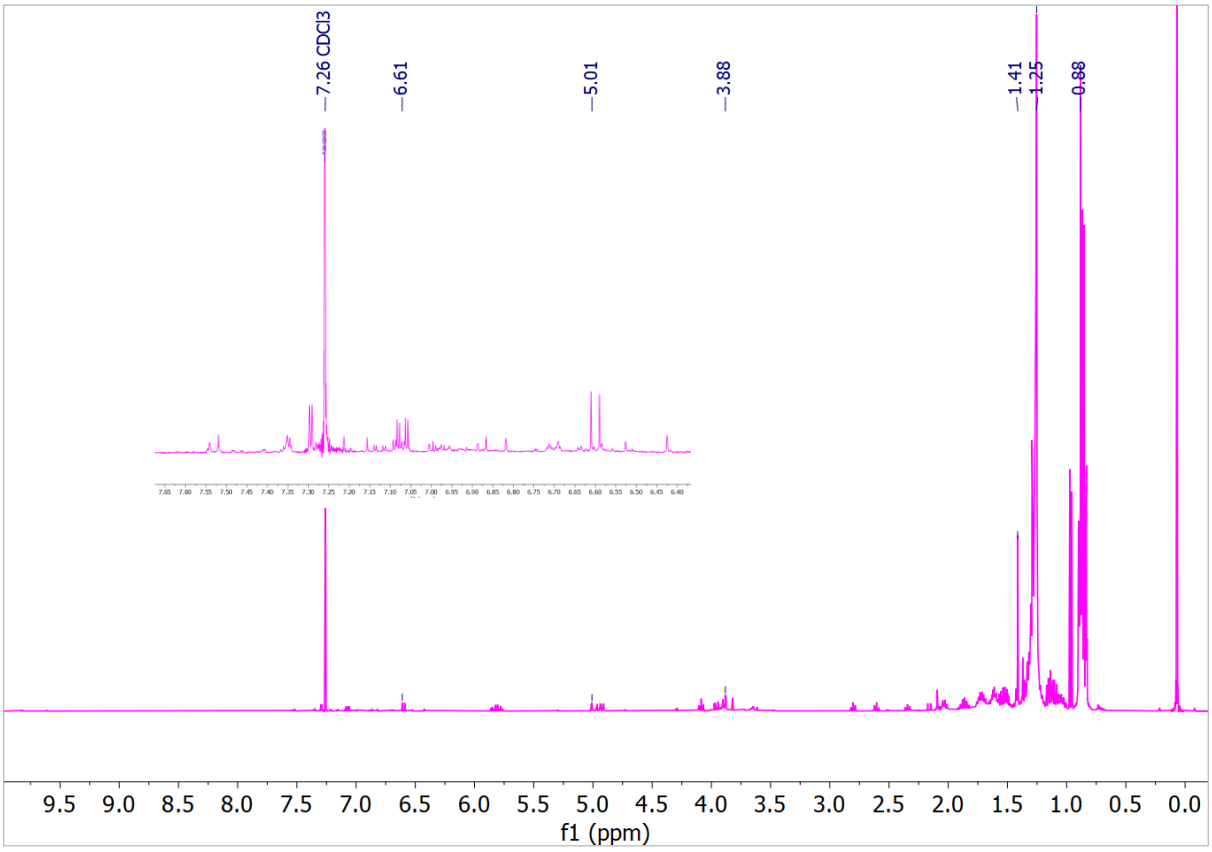

Figure S12: ^{1}H NMR of fraction **5** in $CDCl_3$.

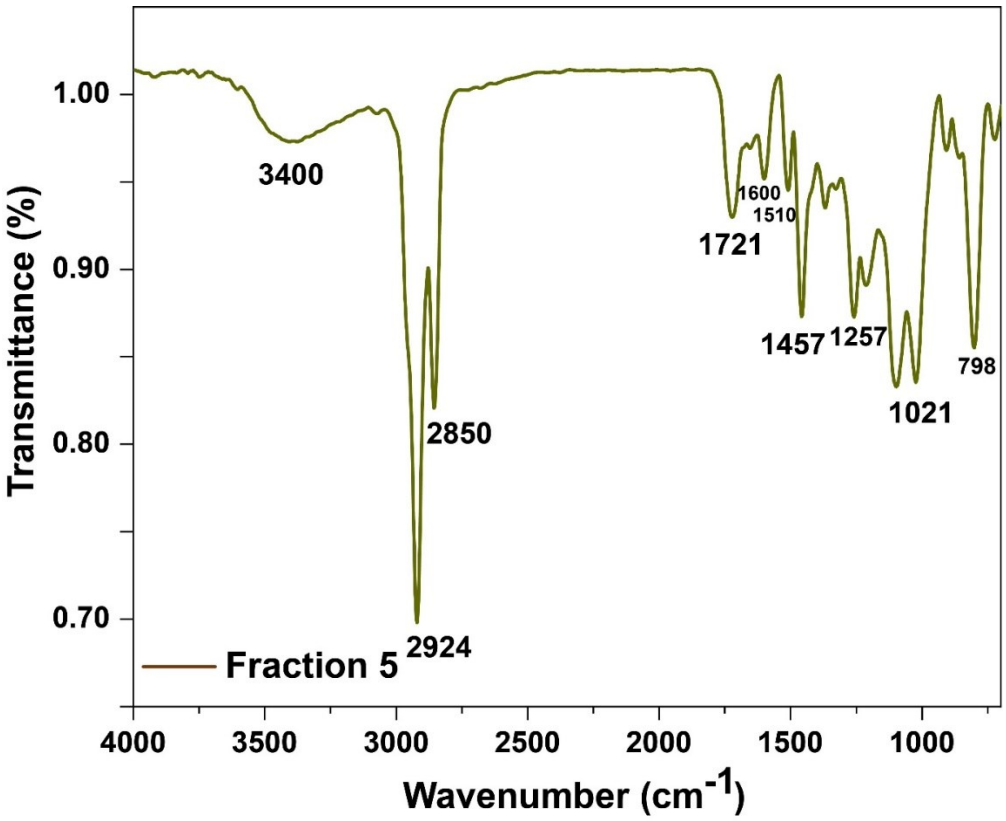

Figure S13: ATR-FTIR of fraction **5** in solid state.

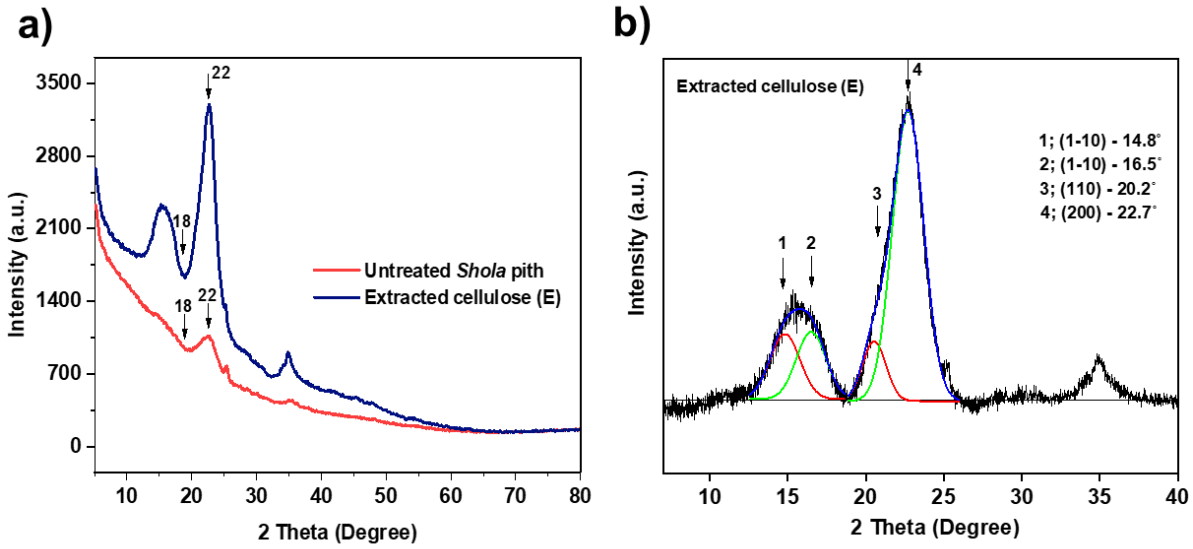

Figure S14: (a) PXRD of the untreated ***Shola* pith** and extracted **cellulose,** (b) **Deconvoluted PXRD spectrum** of extracted cellulose.

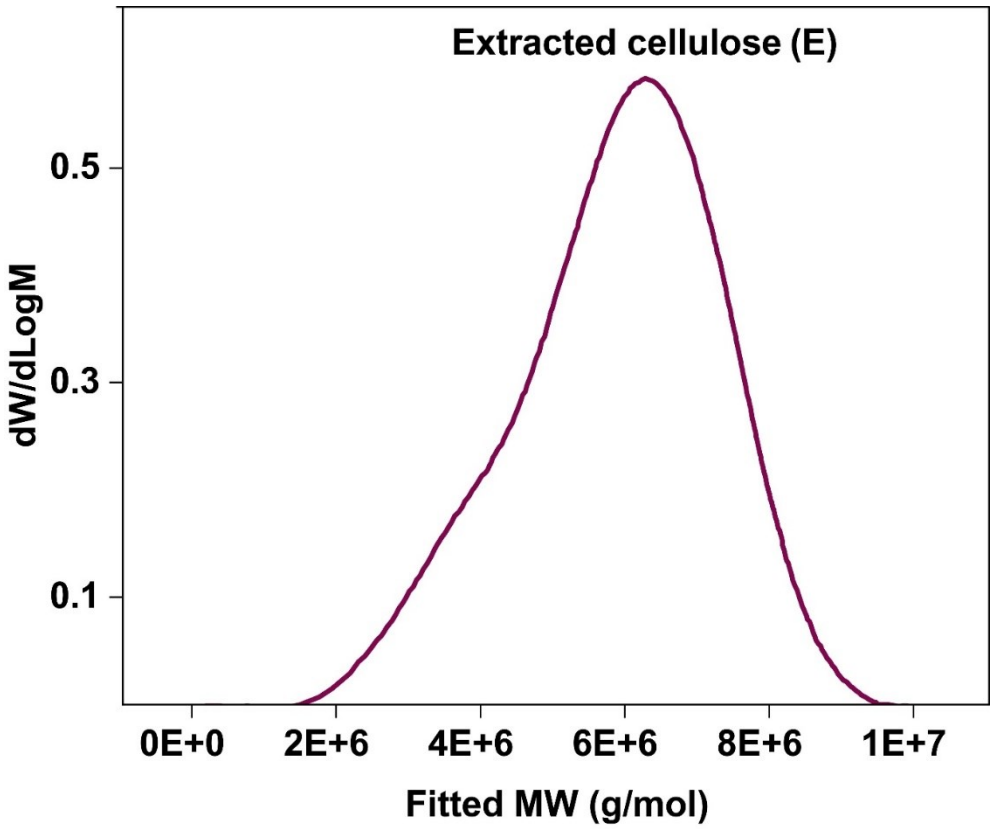

Figure S15: GPC of extracted **cellulose (E).**

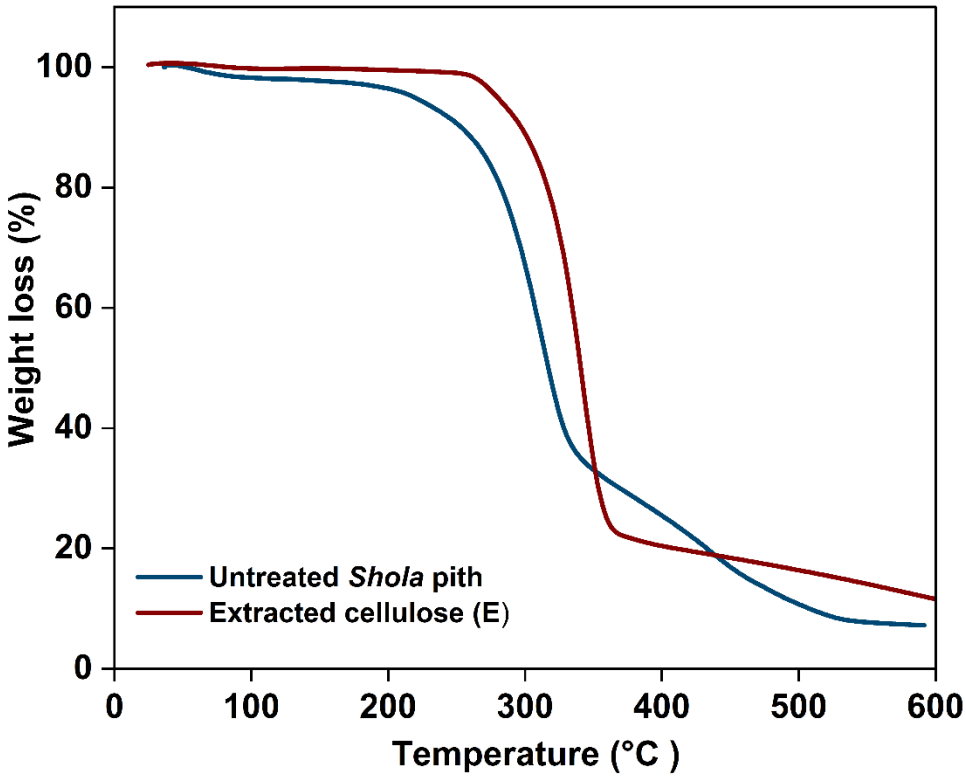

Figure S16: TGA of the untreated ***Shola*** **pith** and extracted **cellulose**.

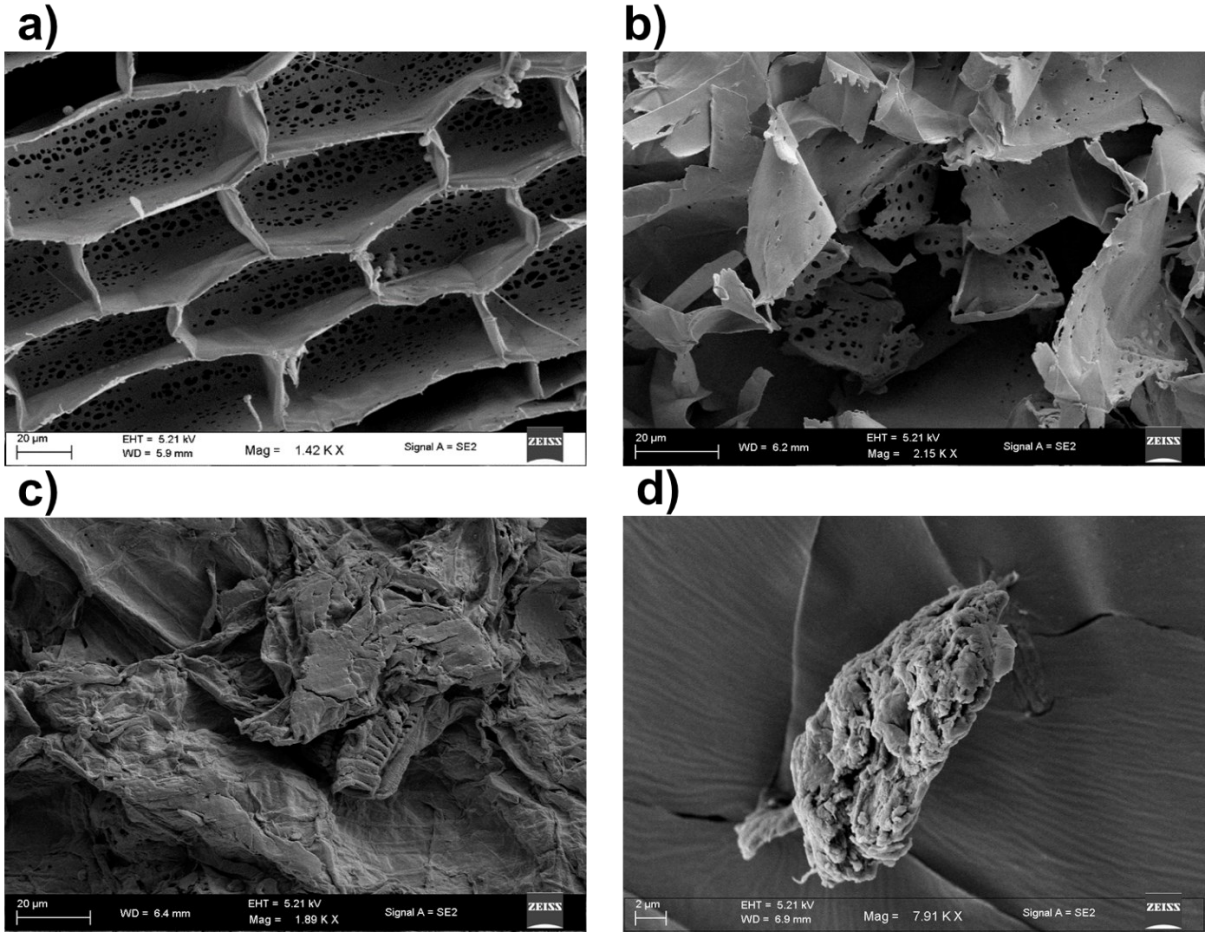

Figure S17: (a) SEM images of the **intact native *Shola* pith**, (b) SEM images of the native **ground *Shola* pith**, (c) SEM images of the **extracted cellulose** (fraction **E**), (d) SEM images of the native **ball-milled** *Shola* pith.

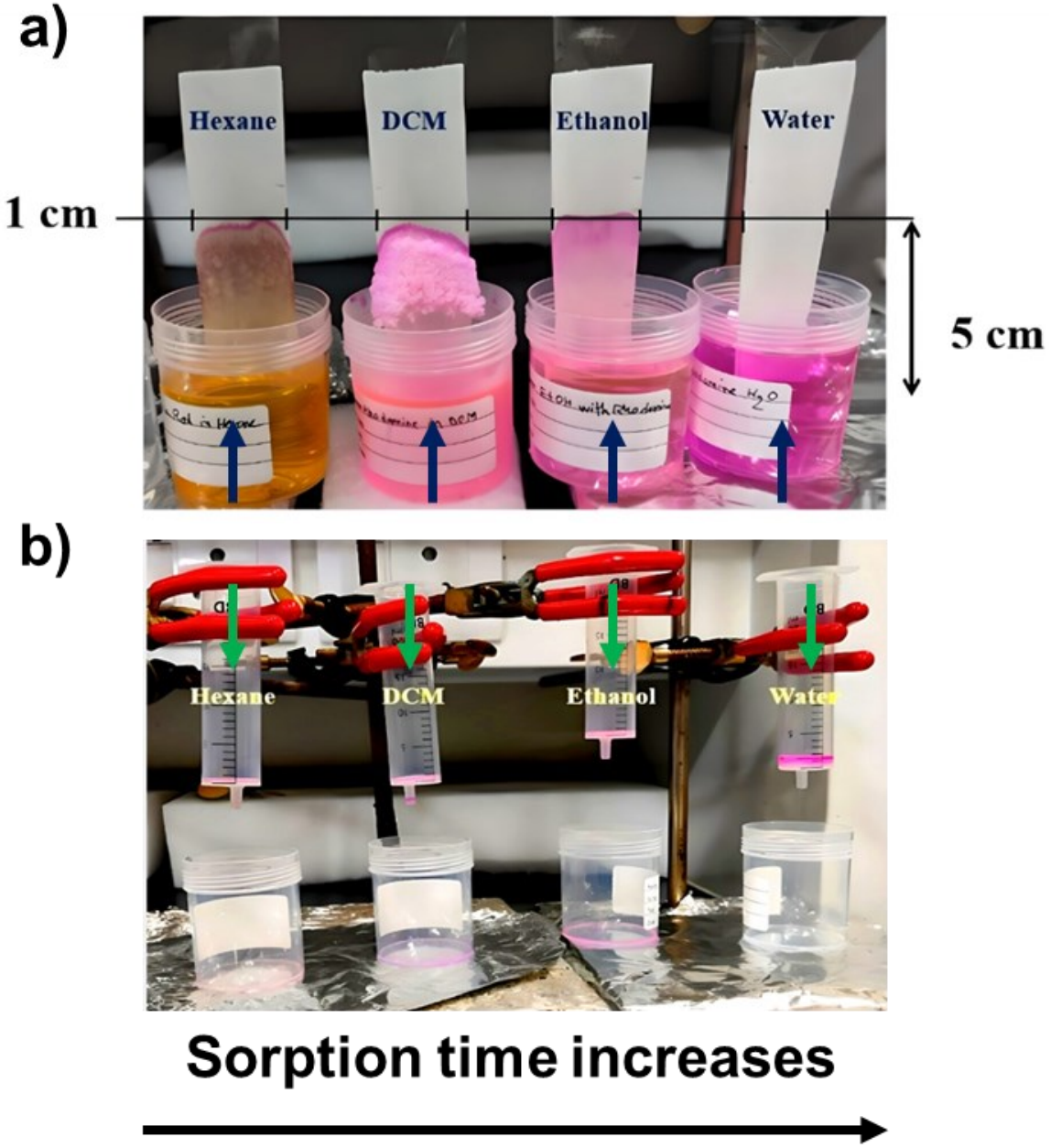

Figure S18: (a) **The capillary action behaviour** of hexane, DCM, ethanol, and water in the *Shola* pith, (b) **The gravimetry action behaviour** of hexane, DCM, ethanol, and water in the *Shola* pith.

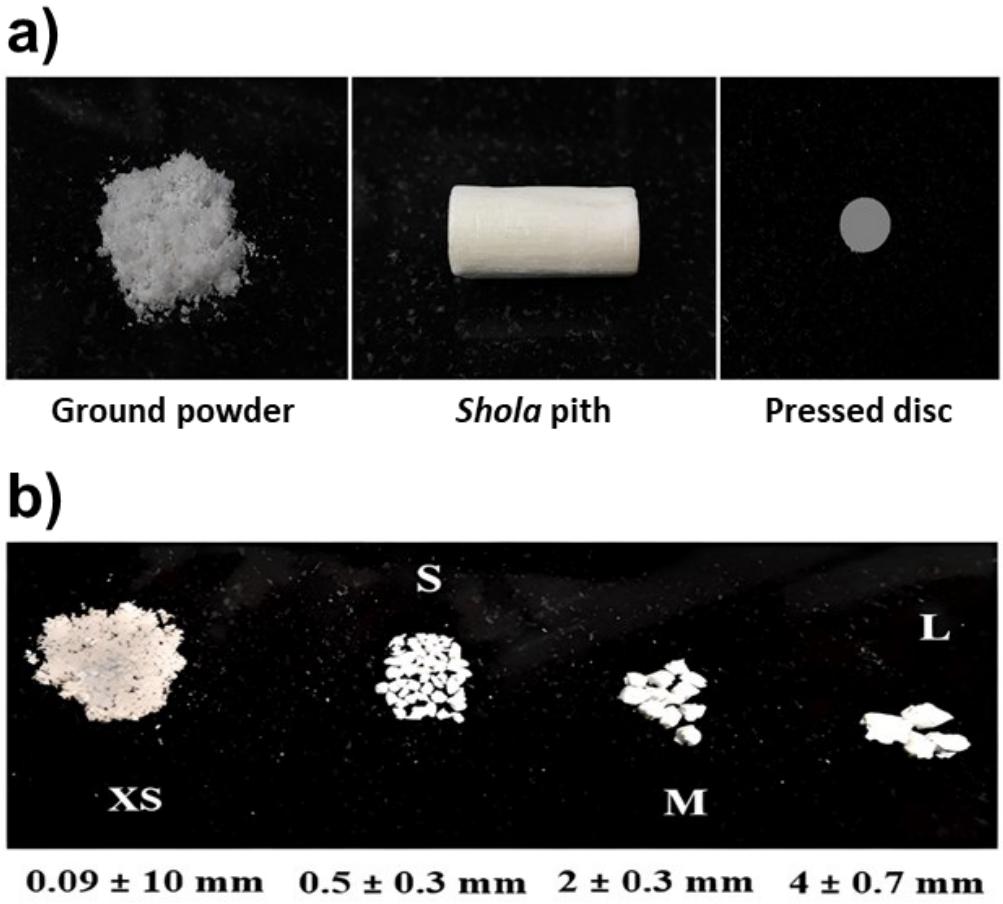

Figure S19. (a) Oil sorption by the *Shola* pith of **different shapes**, (b) Oil sorption by the ground *Shola* pith of **different particle sizes**.

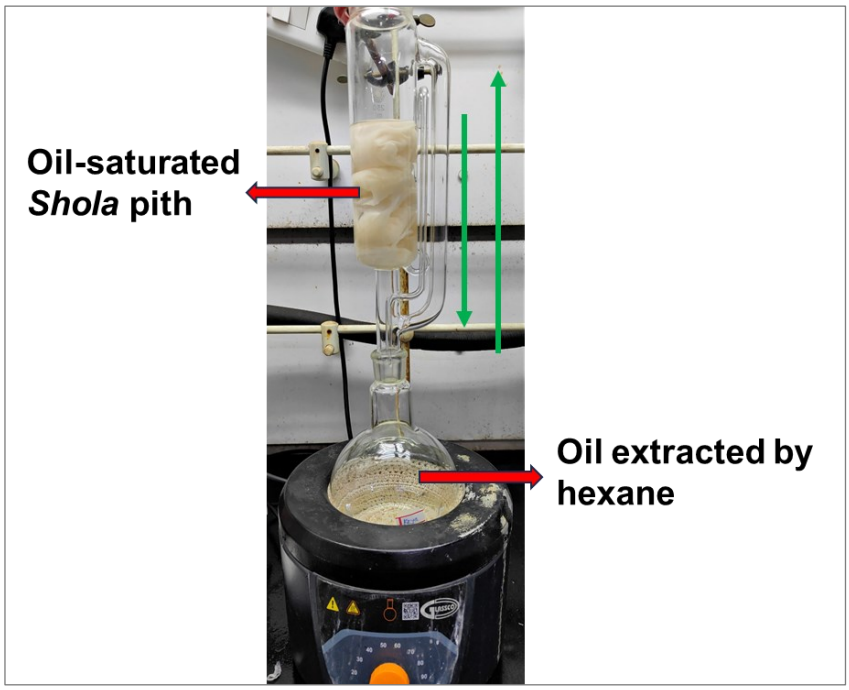

Figure S20. Experimental set-up for **recovery of oil** from the samples by solvent extraction.

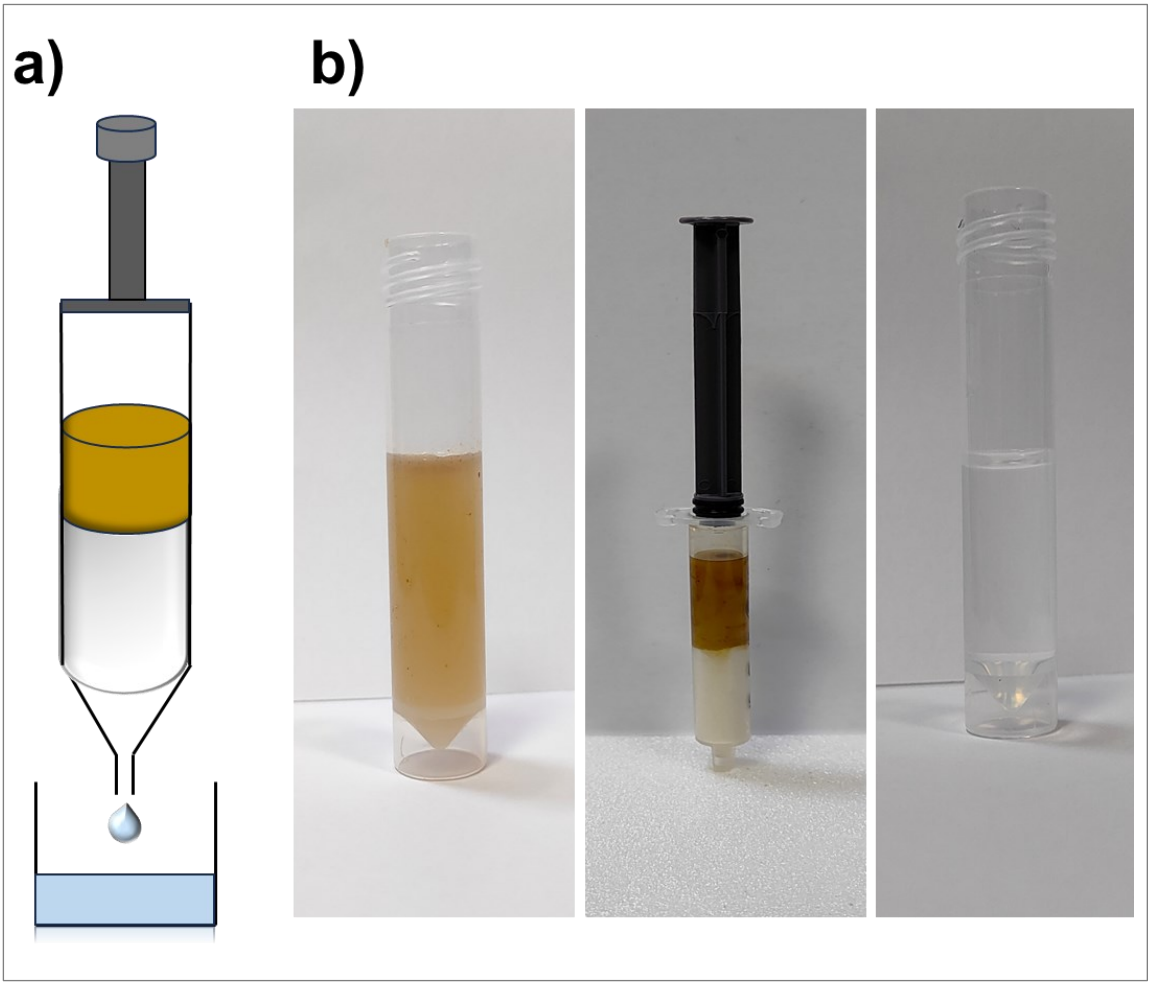

Figure S21. (a) Schematic diagram of oil/water **emulsion separation** with the *Shola* pith packed inside a syringe, (b) Image of **laboratory** experiment (crude oil/water **emulsion, packed** *Shola* pith with the emulsion, and **eluted** water).

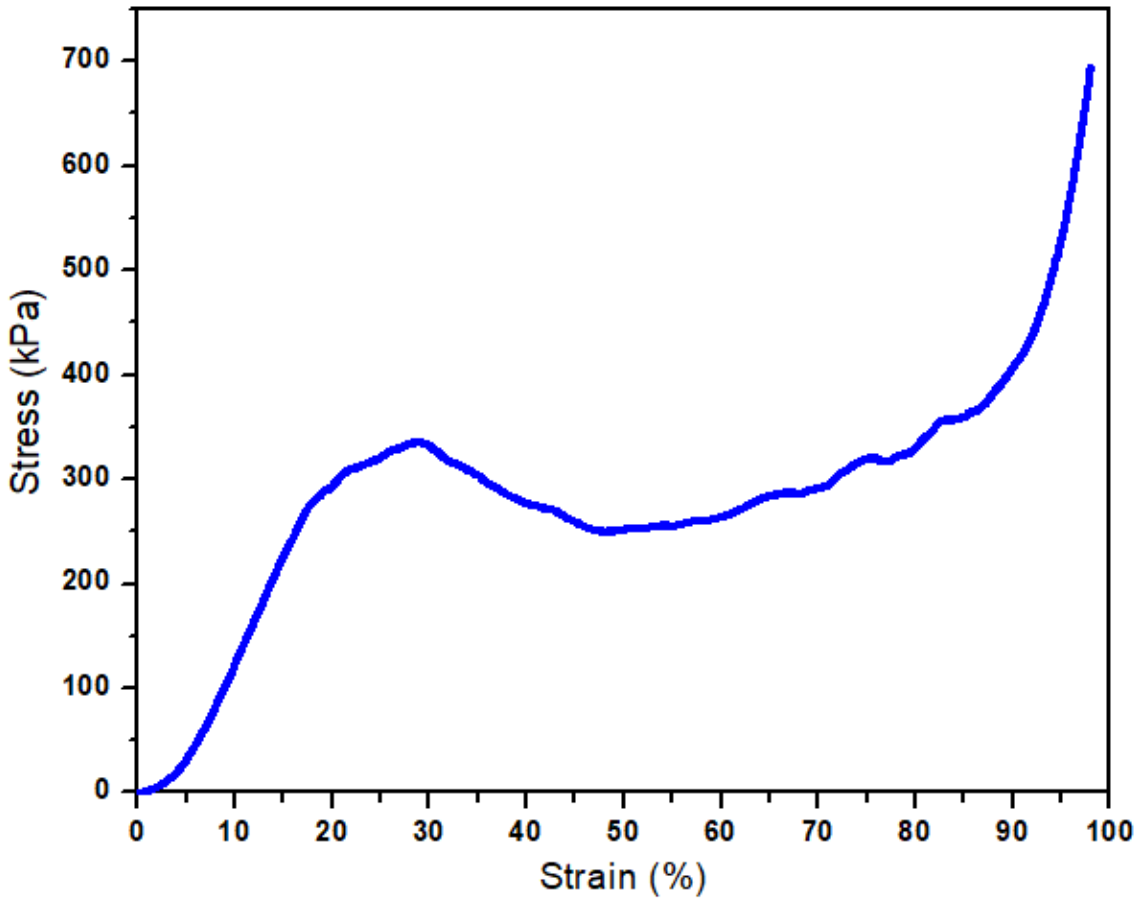

Figure S22. Compressive **stress-strain** curve of the *Shola* pith.

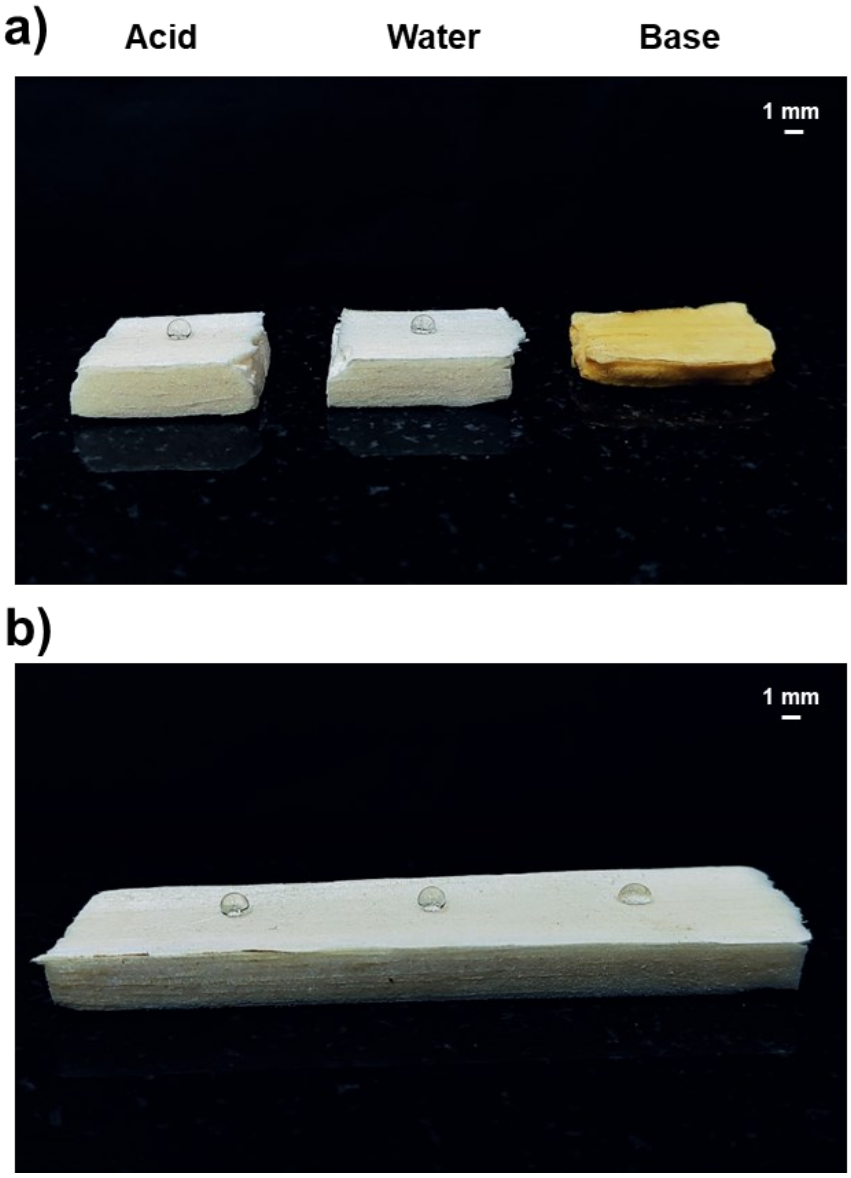

Figure S23. (a) Images of **water droplets** placed on the dried *Shola* pith after dipping in 0.1 N HCl, DI water, and 1 N NaOH, (b) Images of **acid (0.1 N HCl), water, and base (1 N NaOH) droplets** placed on the native *Shola* pith.

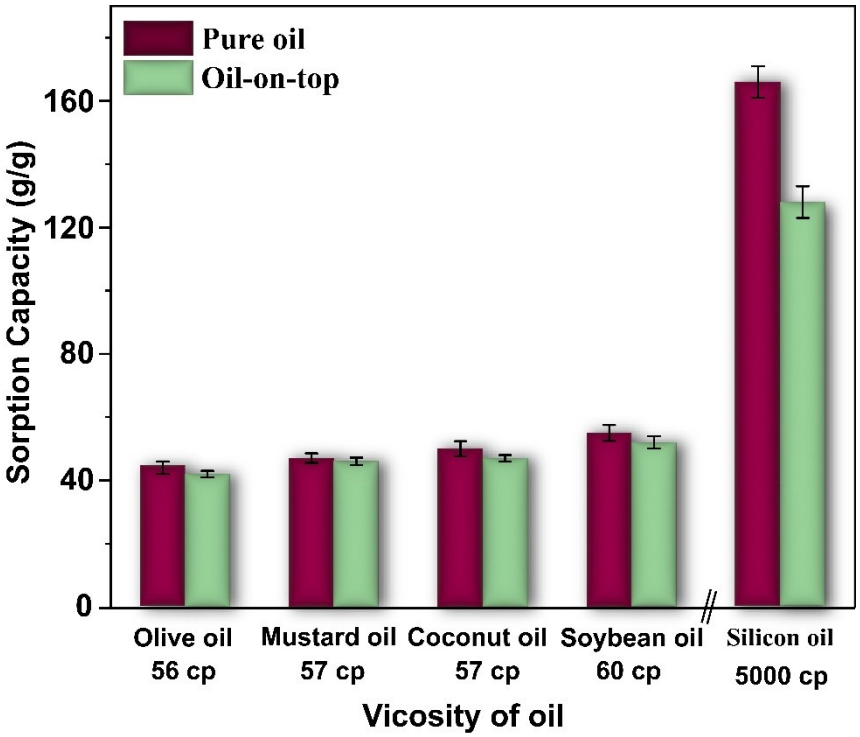

Figure S24. The effect of **oil viscosity** on the oil sorption capacity of the *Shola* pith.

Reference

1 R. Simões, I. Miranda and H. Pereira, *Phytochem Anal*, 2022, **33**, 127–135.
2 A. P. Deshmukh, A. J. Simpson, C. M. Hadad and P. G. Hatcher, *Organic Geochemistry*, 2005, **36**, 1072–1085.
3 A. P. Deshmukh, A. J. Simpson and P. G. Hatcher, *Phytochemistry*, 2003, **64**, 1163–1170.
4 J. A. Heredia-Guerrero, J. J. Benítez, E. Domínguez, I. S. Bayer, R. Cingolani, A. Athanassiou and A. Heredia, 2016, **28** (2).
5 G. Rodríguez-Gutiérrez, F. Rubio-Senent, A. Lama-Muñoz, A. García and J. Fernández-Bolaños, *J. Agric. Food Chem.*, 2014, **62**, 8973–8981.
6 Q. Luo, H. Peng, M. Zhou, D. Lin, R. Ruan, Y. Wan, J. Zhang and Y. Liu, *BioResources*,2012, **7**.
7 Z. Tian, J. Chen, X. Ji, Q. Wang, G. Yang and P. Fatehi, *BioResources*, 2017, **12**, 2609–2617.
8 J. Müller-Maatsch, A. Caligiani, T. Tedeschi, K. Elst and S. Sforza, *J. Agric. Food Chem.*, 2014, **62**, 9081–9087.
9 V. R. Robledo*, L. I. C. Vázquez, V. R. Robledo* and L. I. C. Vázquez, in *Pectins - Extraction, Purification, Characterisation and Applications*, IntechOpen, 2019.
10 F. Wang, C. Du, J. Chen, L. Shi and H. Li, *Polymers (Basel)*, 2021, **13**, 2847.
11 A. Roman-Benn, C. A. Contador, M.-W. Li, H.-M. Lam, K. Ah-Hen, P. E. Ulloa and M. C. Ravanal, *Food Chemistry Advances*, 2023, **2**, 100192.
12 Y. Wang, Y. Yang, Y. Qu and J. Zhang, *Bioresource Technology*, 2021, **337**, 125506.
13 S. Chu, A. V. Subrahmanyam and G. W. Huber, *Green Chemistry*, 2013, **15**, 125–136.
14 S. Kostryukov, P. Petrov, V. TEZIKOVA, Y. MASTEROVA, T. IDRIS and N. KOSTRYUKOV, *Cellulose Chemistry and Technology*, 2021, **55**, 461–468.
15 S. Sarkar, M. Mondal, P. Ghosh, M. Saha and S. Chatterjee, *J. Med. Plants Stud.*, 2020, **8**, 166–170.
16 R. Khandanlou, G. Ngoh and W. T. Chong, *Bioresources*, 2016, **11**.
17 N. Gralén and The Svedberg, *Nature*, 1943, **152**, 625–625.
18 F. D'Acierno, C. A. Michal and M. J. MacLachlan, *Chem. Rev.*, 2023, **123**, 7295–7325.